Biochimica et Biophysica Acta 1817 (2012) 476–488

Contents lists available at SciVerse ScienceDirect

Biochimica et Biophysica Acta

journal homepage: www.elsevier.com/locate/bbabio

Review

Cytochrome *c* oxidase: Charge translocation coupled to single-electron partial steps of the catalytic cycle ☆

Sergey A. Siletsky, Alexander A. Konstantinov *

A.N. Belozersky Institute of Physico-Chemical Biology, Moscow State University, Moscow 119992, Russia

ARTICLE INFO

Article history:
Received 16 June 2011
Received in revised form 9 August 2011
Accepted 10 August 2011
Available online 16 August 2011

Keywords:
Cytochrome oxidase
Proton pumping
Time-resolved electrometric study
Energy transduction
Cytochrome aa_3
Cytochrome ba_3

ABSTRACT

The paper presents a survey of time-resolved studies of charge translocation by cytochrome *c* oxidase coupled to transfer of the 1st, 2nd 3rd and 4th electrons in the catalytic cycle. Single-electron photoreduction experiments carried out with the A-class cytochrome *c* oxidases of aa_3 type from mitochondria, *Rhodobacter sphaeroides* and *Paracoccus denitrificans* as well as with the ba_3-type oxidase from *Thermus thermophilus* indicate that the protonmotive mechanisms, although similar, may not be identical for different partial steps in the same enzyme species, as well as for the same single-electron transition in different oxidases. The pattern of charge translocation coupled to transfer of a single electron in the A-class oxidases confirms major predictions of the original model of proton pumping by cytochrome oxidase [Artzatbanov, V. Y., Konstantinov, A. A. and Skulachev, V.P. "Involvement of Intramitochondrial Protons in Redox Reactions of Cytochrome *a*." FEBS Lett. 87: 180–185]. The intermediates and partial electrogenic steps observed in the single-electron photoreduction experiments may be very different from those observed during oxidation of the fully reduced oxidase by O_2 in the "flow-flash" studies. This article is part of a Special Issue entitled: Respiratory Oxidases.

1. Introduction

Cytochrome *c* oxidase (COX), a terminal enzyme of the respiratory chain of mitochondria and many bacteria, is a key enzyme of aerobic respiration (reviewed, [1–4]). The enzyme catalyzes reduction of molecular oxygen to water and uses the free energy of the reaction to create transmembrane difference of proton electrochemical potential, $\Delta\mu H^+$, as first proposed by Mitchell [5].The electron transfer sequence in COX can be described by a simple scheme:

$$\text{Cyt } c \rightarrow Cu_A \rightarrow \text{heme } a \rightarrow [\text{heme } a_3, Cu_B] \rightarrow O_2$$

where heme a_3 iron and an "invisible" ion of Cu_B located within ca 4.5 A from each other form a dioxygen-reducing center, where heme iron serves as an anchor for oxygen during O_2 reduction to 2 H_2O molecules, whereas Cu_B serves a redox-dependent gate for oxygen passage to heme a_3 and is involved in electron transfer to oxycomplex of heme a_3.

The catalytic cycle of cytochrome oxidase is depicted in a simplified way in Fig. 1 and shows clear homology to the catalytic cycles of P450 and peroxidases [6–9]. The overall $4e^-$ reaction is comprised of two halves with quite different chemistry. The first two electrons reduce Cu_B and heme a_3 allowing the O_2 molecule to enter the catalytic site and bind to the reduced heme iron, forming an oxycomplex, usually referred as intermediate A. The ferrous–oxy complex is however better described as **S**uperoxo-ferric state [8–10] and is denoted in Fig. 1 as Compound **S** (equivalent to Compound III of peroxidases). Delivery of a second electron from Cu_B to the bound superoxide forms a ferric-**P**eroxy state (**P**). Binding and two-electron reduction of molecular oxygen to peroxide is a classical oxidase reaction in enzymology and this half of the cycle is denoted as *eu-oxidase* to distinguish it from the overall $4e^-$ oxidase reaction [8]. Subsequent asymmetric addition of 2 protons to bound peroxide generates a transient ferric-dihydroperoxy state $\mathbf{P_0}$ analogous to Compound 0 of peroxidases and from here the reaction enters the second half that is fully analogous to the oxidations catalyzed by peroxidases, cytochrome *c* peroxidase in particular. The O—O-bond in $\mathbf{P_0}$ is cleaved heterolytically to form the first water molecule and Compound I-type ferryl intermediate $\mathbf{F_I}$ (still referred in the literature as "peroxy" complex "$\mathbf{P_M}$") with the second electron vacancy located at an aromatic amino acid residue, currently thought to be Tyr244 (bovine numbering). $\mathbf{F_I}$ is reduced sequentially by the 3rd and 4th electrons delivered one by one from cytochrome *c* or an artificial donor first to Compound II-type ferryl intermediate $\mathbf{F_{II}}$ (referred usually as **F** or $\mathbf{F_{580}}$) and then to the oxidized state. The peroxidase half of the catalytic cycle can be followed separately on a multiple turnover basis as partial reaction bypassing the eu-oxidase phase of the cycle [11,12].

To understand the mechanism by which COX reduces oxygen and couples this reaction to generation of membrane potential, $\Delta\psi$, and transmembrane proton activity difference, ΔpH, it is important to

Abbreviations: COX, cytochrome oxidase; BNC, binuclear center; ET, electron transfer; PLS, proton loading site

☆ This article is part of a Special Issue entitled: Respiratory Oxidases.

* Corresponding author. Tel.: +7 495 939 55 49; fax: +7 495 939 31 81.
E-mail address: konst1949@gmail.com (A.A. Konstantinov).

0005-2728/$ – see front matter © 2011 Elsevier B.V. All rights reserved.
doi:10.1016/j.bbabio.2011.08.003

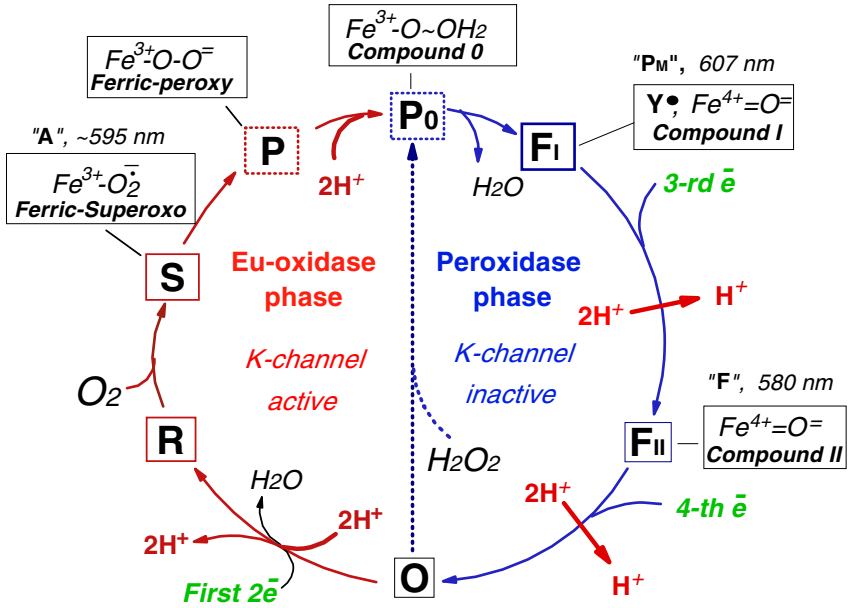

Fig. 1. Catalytic cycle of cytochrome *c* oxidase. Modified from Ref. [8,105] (see the text). Alternative abbreviations commonly used in the literature are indicated for the intermediates **S**, $\mathbf{F_I}$ and $\mathbf{F_{II}}$ ("**A**", "$\mathbf{P_M}$" and "**F**", respectively) as well as the characteristic absorption maxima of the intermediates in the difference spectra. The intermediates **P** (ferric-peroxy) and $\mathbf{P_0}$ (Compound 0, ferric-dihydroperoxy) have not been observed experimentally but are likely to be formed transiently by analogy with other hemoproteins like P450s or peroxidases [6–9,106] and are shown in dotted boxes. The two protons required for heterolytic cleavage of the O—O bond in the ferric-peroxy intermediate **P** are assumed to be delivered via/from the K-channel [8,9,23,105,107]. Proton pumping events in the eu-oxidase part of the catalytic cycle are not yet fully clear because the chemical differences between the multiple forms of the oxidized and singly-reduced forms of the enzyme have not been firmly established. Therefore, specifying the individual proton pumping steps in the eu-oxidase part of the cycle is deliberately eluded.

resolve different steps in the catalytic cycle and investigate each of these steps. In this paper we review time-resolved studies of intraprotein charge translocation coupled to different single-electron steps of the catalytic cycle.

1.1. Single electron photoreduction and oxidation by O_2 ("flow-flash" studies)

There are two very different approaches towards the time-resolved studies of charge translocation by COX. In this group, a method combining time-resolved electrometric measurements with flash-induced injection of a single electron into Cu_A of COX poised at different initial redox states was developed [13]. Subsequently, time-resolved electrometric measurements were combined in Helsinki group with the so called "flow-flash" technique [14] and electrogenic steps coupled to oxidation of the fully reduced COX by oxygen were studied extensively. Some of the intermediates formed during oxidation of the fully reduced COX by oxygen are specific for this experimental approach and may be different from the intermediates formed during the aerobic turnover of the enzyme passing through the 2-electron reduction of the binuclear site (Fig. 1), as well as from the intermediates studied in the single-electron photoreduction experiments. In this review we focus mainly on single-electron photoreduction experiments. A survey of time-resolved electrometric measurements of single-electron transitions of the enzyme is presented and significance of these measurements for elucidation of the protonmotive mechanism of the enzyme is discussed. The kinetics of charge translocation by COX during oxidation of the fully reduced enzyme by O_2 may be discussed elsewhere in this volume.

1.2. Questions to be addressed

In the paper we would like to draw attention to the following questions.

(i) May the electrogenic reactions in the single-electron photoreduction studies be different from those studied in the flow-flash experiments during oxidation of the fully reduced COX?

(ii) Are the protonmotive mechanisms the same or different for different single-electron steps of the catalytic cycle in the same enzyme species?

(iii) Are the protonmotive mechanisms identical for the same catalytic steps in the A-type oxidases from mitochondria and bacteria? (see [15] for definition of the A, B and C classes of heme-copper oxidases).

(iv) What are the differences between the protonmotive mechanisms in the fully pumping A-type and partially pumping B-type oxidases?

2. Protonmotive mechanism of cytochrome oxidase: from redox loop to proton pump

Cytochrome oxidase was proposed originally to generate $\Delta\psi$ and ΔpH by carrying out transmembrane electron transfer (ET) from cytochrome *c* at the outer face of the membrane to heme a_3 located at the inner face of the membrane, where oxygen is reduced to water, consuming protons from the inner aqueous phase (redox loop scheme) [5]. The model predicted transmembrane transfer of 4 electric charges per O_2 reduced, and presumed that (1) heme a_3 is located at the inner side of the membrane and (2) heme *a* is a purely electron carrier, located in the middle of the membrane.

While trying to test these postulates, it was found that reduction of heme *a* is coupled to proton uptake from the inner aqueous phase [16,17]. At the same time Wikstrom reported [18] that O_2 reduction by COX is accompanied by appearance of protons at the outer side of the mitochondrial membrane with a stoichiometry of $H^+/e^- = 1$, i.e. that COX operates as a proton pump translocating two charges across the membrane per each electron transferred to oxygen.

Combining the two findings, a detailed model of cytochrome oxidase protonmotive mechanism was suggested in 1977/1978 [17,19] explaining transmembrane translocation of two electric charges coupled to transfer of a single electron through the enzyme (Fig. 2). The model proposed that: (1) ET from heme *a* to heme a_3 occurs along rather than across the membrane and is not per se electrogenic; and (2) there are

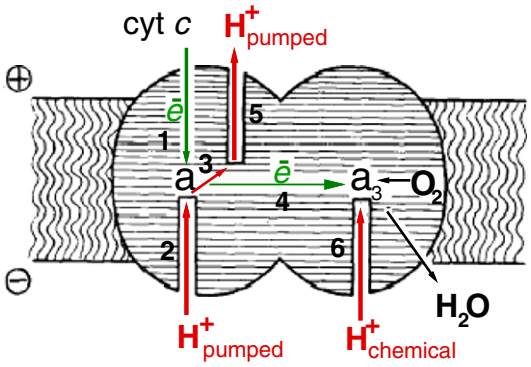

Fig. 2. Original model of cytochrome oxidase protonmotive mechanism coupled to transfer of a single electron through the enzyme [17,19]. The originally postulated sequence of events is denoted in Fig. 2 by numbers near the arrows: (1) the initial electrogenic electronic phase associated with vectorial e^- transfer to heme *a* postulated originally by Mitchell; (2) electrogenic uptake of the pumped proton from the N-phase; (3) translocation of the pumped proton from the bottom of the input well to the bottom of the exit well (in modern words for the $\mathbf{F_H \rightarrow O}$ step in *R. sphaeroides* COX, proton transfer from E286 at the bottom of the D-channel to the so-called "proton loading site" (PLS)) gating non-electrogenic electron transfer from heme *a* to heme a_3; (4) ET from heme *a* to the binuclear site; (5) release of the pumped proton to the outside; (6) uptake of the chemical proton from the N-phase. The first time-resolved measurements of $\Delta\psi$ generation [13] showed however that the major phases of electrogenic proton transfer match kinetically oxidation of heme *a* rather than its reduction [13]. According to current thinking, two changes are to be made to the sequence of the events in Fig. 2 (see Fig. 5). First, step 3 (internal proton transfer from E286 to PLS) is likely to precede step 2 (uptake of the pumped proton); i.e., following heme *a* reduction, E286 is first deprotonated at step 2 and *then* takes up H^+ from the N-phase at step 3. Second, step 5 (release of the pumped proton from PLS to the outside) is thought to follow step 6 (delivery of the chemical proton) as proposed originally by P.R. Rich [62]. I.e., the currently presumed sequence will be $1 \rightarrow 3 \rightarrow 2 \rightarrow 4 \rightarrow 6 \rightarrow 5$. It is noted that, in fact, the steps 2, 3, 4 are likely to merge as well as the steps 5, 6 forming two clusters of concerted electrogenic events. The individual steps within the clusters are not resolved kinetically under normal conditions. Finally, water formed from O_2 is now thought to be released to the outer aqueous phase [23,24] rather than to the matrix as was depicted in the original scheme [17,19].

special structural domains called proton channels or proton wells [5,20] which enable electrostatic coupling of ET between the hemes to electrogenic proton transfer, providing for generation of $\Delta\psi$ and proton pumping. Two input and one exit proton channels were proposed to be involved in electrogenic translocation of the pumped and chemical protons by COX coupled to ET through the redox centers. These predictions on the structure of COX were largely confirmed when the 3D structure of the enzyme was solved [21,22], except that the exit proton pathway does not involve a typical proton-conducting channel structure, like in the case of the K- or D-input proton channels, but rather is organized as a network of hydrogen-bonded protein groups and water molecules with several potential proton exit trajectories identified [23–25] (and see also [4] for a fully different proton exit pathway proposed for mammalian oxidase).

Besides the predictions on the structure of COX, the model in Fig. 2 made several explicit postulates concerning the function of the enzyme:

(1) Transfer of an electron through the enzyme should be coupled to multiple partial charge transfer steps. Some of the steps would be coupled to vectorial ET from Cu_A to heme *a*, and besides there should be at least 2 or 3 electrogenic phases, corresponding to uptake of the pumped and chemical proton from the *N*-phase and to release of the pumped proton to the outside. Conceivably, some of the partial charge translocation steps can be coupled to each other merging into a single concerted step.
(2) Internal transfer of the pumped proton from the bottom of the input proton well to the bottom of the output proton well gates ET from heme *a* to heme a_3.
(3) Uptake of the pumped proton precedes uptake of the chemical proton.

These predictions served as a roadmap for investigations into the mechanism of charge translocation by COX in this group as described below.

3. Charge transfer steps linked to reduction of heme *a* and to its oxidation by the binuclear site

As mentioned above, the model in Fig. 2 postulates that transfer of a single electron through the enzyme should give rise to several partial steps of charge translocation, some coupled to reduction and some to reoxidation of heme *a*. To test this prediction, a method was developed allowing to time-resolve partial steps of charge transfer across the membrane in liposome-reconstituted cytochrome oxidase. Ru(II)–tris-bipyridyl complex (RuBpy) was used as a photoactivated single-electron donor for Cu_A [26] in combination with time-resolved electrometric technique developed originally in this institute by Drs. L.A. Drachev and A.D.Kaulen to monitor rapid kinetics of $\Delta\psi$ generation by bacteriorhodopsin [27,28] and by photosynthetic enzymes [29,30]. With the aid of this method implemented subsequently in three other laboratories (the Helsinki, Frankfurt and Stockholm groups), the kinetics of charge translocation across the membrane coupled to transfer of the 1st [13,31–37], 2nd [35,38], 3rd [31,36,39] and 4th electrons [13,31,38,40–42] in the catalytic cycle of COX was studied for the mammalian enzyme and several bacterial cytochrome oxidases.

The first single-electron photoreduction experiments were made for the $\mathbf{F_H \rightarrow O}$ transition in liposome-reconstituted bovine oxidase [13] and established a generic pattern of charge translocation observed subsequently for the $\mathbf{F_H \rightarrow O}$ transition in bacterial oxidases [38,40] as well as for other single-electron steps of the catalytic cycle [31,36,38,39]. The electrogenic response coupled to single-electron photoreduction of COX is typically comprised of two parts, one associated with very rapid (μs) reduction of heme *a* by Cu_A and the other with subsequent much slower (ms) re-oxidation of heme *a* by the binuclear site. These two parts are well resolved in time, but they can also be clearly separated by their sensitivity to KCN that prevents oxidation of heme *a* by the binuclear site, but does not inhibit heme *a* reduction.

The magnitude ratio of the charge translocation phases linked to the reduction and oxidation of the low-spin heme *a* (heme *b* in ba_3 oxidase from *Thermus thermophilus*) vary significantly depending on the enzyme species and the catalytic step studied, as summarized in Table 1. The variation may indicate different number of protons translocated during oxidation of heme *a* by the binuclear site in the enzymes with impaired proton pumping (e.g., non-pumping N139D mutant oxidase from *R. sphaeroides*) but also may report altered distribution of the partial electrogenic steps between the heme *a* reduction and heme *a* oxidation phases in the fully pumping oxidases (e.g., cf. the $\mathbf{F_H \rightarrow O}$ transitions in the mitochondrial and bacterial A-class oxidases). Together with the magnitude ratio of the two protonic phases resolved within the KCN-sensitive part of the response, these data give a kind of crude electric portrait of a particular single electron transition. We will return to discussion of these values below.

4. Electrogenic events coupled to transfer of the 1st, 2nd, 3rd and 4th electrons in the A-class oxidases: a survey of experimental data

Below we discuss characteristics of charge translocation coupled to different individual single-electron steps of the catalytic cycle in the order of the data completeness.

4.1. Transfer of the 4th electron. The $\mathbf{F_H \rightarrow O}$ *transition*

This is probably the single-electron step studied in most detail. Experiments were done with oxidase from bovine heart, as well as with

Table 1
Magnitude ratio of the electrogenic phases coupled to reduction (KCN-insensitive) and oxidation (KCN-sensitive) of the low-spin heme.

Object, transition, reference	Parts of the electrogenic response coupled to the reduction and oxidation of heme *a* (or heme *b* for ba_3 oxidase)			
	A coupled to reduction of heme *a* (KCN-insensitive part), %	B coupled to ET from heme *a* to the binuclear site (KCN-sensitive, part), %	Magnitude ratio	
			A:B	B_1/B_2 (protonic 1/protonic 2)
aa_3 from bovine heart				
1st *e* (**O→R**^{1})	100	0	n/a	n/a
3rd *e* (**F_I→F_{II}**) [31,39]	21	79	1:3.8	0.84
4th *e* (**F_{II}→O**) [13,31,39]	20	80	1:4	0.86
aa_3 from R. sphaeroides, WT				
3 rd *e* (**F_I→F_{II}**) [39]	28	72	1:2.6	2.3
4th *e* (**F_{II}→O**) [40,41]	30	70	1 : 2.3	0.89
aa_3 from R. sphaeroides, non-pumping mutant N139D				
4th *e* (**F_{II}→O**) [41]	~40	~60	~1:1.5	n/a, single protonic pase
aa_3 from P. denitrificans, WT				
1st *e* (**O→R**^{1}) [35]	~100	~0	n/a	n/a
1st *e* (**O→R**^{1}) [33]	~60	~40	1:0.67	n/a, single protonic phase
1st *e* (“**O_H**”→**R**^{1}) [37] [a]	~17	~83	~1:4.9	~0.9
1st *e* (“**O_H**”→**R**^{1}), data from [37] re-analyzed in [69]	17–21	83–79	1:3.9–1:4.9	~0.9
2nd *e* (**R**^{1}→**R**^{2}) [38]	26	74	1:2.9	0.74 [b]
3 rd *e* (**F_I→F_{II}**) [36][a]	~17	83	1:4.9	2.2
4th *e* (**F_{II}→O**) [38]	30	70	1:2.3	0.82[b]
ba_3 from T. thermophilus				
1st (**O→R**^{1}) [32], as observed	60	40	1 : 0.67	n/a
1st (**O→R**^{1}) [32], corrected [c]	~30	~70	~1:2.3[c]	n/a
3th (“**F_I→F_{II}**”) [32][d]	31	69	1:2.2	0.5

[a] Original data have been corrected for complete electron dislocation from Cu_A to heme *a*.
[b] Re-calculated from the original data assuming serial sequence of the protonic phases [39] (Eqs. (1), (2) in this paper).
[c] Corrected for incomplete ET from heme *b* to heme a_3 (K_{eq} = 0.43) [82]);
[d] Calculated from the original data at 40 mM H_2O_2.

the wild type and mutant forms of COX from *R. sphaeroides* and *P. denitrificans*. Studies of the **F_{II}→O** transition benefit from simple experimental design. The solubilized or membrane-bound oxidized enzyme can be fully converted to the stable ferryl-oxo state by addition of excess hydrogen peroxide [43–45] and in this state, ferryl-oxo complex of heme a_3 is a sole ultimate acceptor for the photoinjected electron. This allows for simple and straightforward interpretation of the data, not complicated by multiplicity of the initial and final states inherent in some other transitions. If not stated otherwise, all the experiments discussed below refer to pH = 8.

4.1.1. Mitochondrial oxidase

Initially, time-resolved electrometric studies of the the **F_{II}→O** transition were made with the mitochondrial oxidase from bovine heart [13]. Photoinjection of a single-electron from RuBpy into bovine COX poised at the ferryl-oxo state **F_{II}** converts the enzyme to the oxidized (ferric) form and gives rise to 3 major electrogenic phases associated with reduction (rapid phase) and reoxidation (intermediate and slow phases) of heme *a*. Characteristics of the electrogenic steps coupled to the **F_{II}→O** transition in liposome-reconstituted bovine COX at pH 8 are summarized in Table 2.

The first electrogenic phase, often referred as *rapid*, has τ_1 of ~40–50 μs. Experiments with a photoactive Ru-labeled cytochrome-derivative as a more native electron donor [46] yielded the same value of rate constant for the rapid phase. The KCN-insensitive rapid phase of $\Delta\psi$ generation is followed in bovine oxidase by two phases with τ_2 = 1.2 ms (*intermediate* phase, or protonic phase 1) and τ_3 = 4.5 ms (*slow* phase, or protonic phase 2) (Table 2). These slower electrogenic steps are prevented by KCN and originate in vectorial proton transfer coupled to reoxidation of heme *a* by the ferryl-oxo complex of heme a_3. The slow phase of the electric response (protonic phase 2) is decelerated 6–7-fold by 100 μM Zn^{2+} added from the outside [47].

The magnitude ratio of the two protonic phases as observed is ~1:3 [13]. However, if the two protonic phases occur in series rather than in parallel (which is likely to be the case), and if their rate constants, k_2 and k_3, differ by less than an order of magnitude, the true magnitude

Table 2
Charge translocation phases coupled to **F_{II}→O** transition in bovine oxidase.

Electrogenic phase	Time constant	Contribution			Electron transfer events
		As observed [13]	Recalculated assuming serial sequence of the protonic phases [39]	Charges across the membrane	
Rapid	45 μs	20%	20%	0.40	Cu_A→heme *a* ET
Intermediate (protonic 1)	1.2 ms	20%	37%	0.74	Heme *a*→heme a_3 ET (75–90%)
Slow (protonic 2)	4.5 ms	60%	43%	0.86	Minor residual ET phase
		Σ = 100%	Σ = 100%	Σ = 2	

Table 3
Characteristics of the electrogenic phases coupled to $\mathbf{F_{II}} \rightarrow \mathbf{O}$ transition in bovine oxidase.

Electrogenic phase	pH-dependence[a]	D_2O/H_2O solvent KIE	Temperature dependence (E_{act})[b]
Rapid	None	1.0	3.6 kcal/mol
Intermediate (protonic 1)	None	1.7 ± 0.3	19.4 kcal/mol
Slow (protonic 2)	Decelerates above 7.5 with pK ~ 9.3	2.1 ± 0.3	16.7 kcal/mol

[a] Data drom [49,51].
[b] Data from [50,51].

values, A_2 and A_3, need to be calculated from the observed values, $A_{2(obs)}$ and $A_{3(obs)}$, according to the Eqs. (1) and (2) [39,48]:

$$A_2 = A_{2(obs)} + A_{3(obs)} \times k_3 / k_2 \quad (1)$$

$$A_3 = A_{3(obs)} \times (k_2 - k_3) / k_2. \quad (2)$$

The calculations show that, in fact, the two protonic phases have similar magnitudes ($A_2/A_3 = 0.86$) (Tables 1 and 2). The $\mathbf{F_{II}} \rightarrow \mathbf{O}$ transition of COX is currently thought to be coupled to translocation of 2 electric charges across the membrane. With this assumption, the absolute electrogenicities of the time-resolved electrogenic phases in bovine oxidase (number of charges translocated across the membrane) can be estimated as shown in Table 2.

Additional characteristics of the electrogenic phases such as temperature and pH-dependences as well as H_2O/D_2O kinetic solvent isotope effect (KIE) [49–51] are shown in Table 3.

4.1.1.1. Attribution of the electrogenic phases. The rapid phase is KCN-insensitive, and therefore does not include components associated with ET to the binuclear site. It matches kinetically electron transfer from Cu_A to heme *a* [13,26,52], shows a very weak temperature dependence (activation energy of 3.6 kcal/mol) that coincides with that of ET from Cu_A to heme *a* [53,54], does not depend on pH and is not affected by H_2O/D_2O-replacement (Table 3). Consequently the rapid electrogenic phase is commonly assigned to vectorial electron transfer from Cu_A to heme *a*, a process postulated originally by Mitchell [55,56]. A phase with very similar characteristics is inherent in the kinetics of charge translocation coupled to the $\mathbf{O} \rightarrow \mathbf{R}^1$ and $\mathbf{F_I} \rightarrow \mathbf{F_{II}}$ steps of the catalytic cycle in bovine COX [31].

The KCN-sensitive part of electrogenic response is obviously comprised of proton transfer steps coupled to ET from heme *a* to the binuclear site and to chemistry of oxygen reduction at heme a_3. Both protonic phases reveal moderate H/D solvent kinetic isotope effect (KIE) with rather close values of 1.7 ± 0.3 for the intermediate and 2.1 ± 0.3 for the slow phase (Table 3). At the same time, the pH dependences of the two phases are quite different. The rate of protonic phase 2 decreases at pH > 8, consistent with the pH-dependence of proton uptake in the $\mathbf{F_{II}} \rightarrow \mathbf{O}$ transition in the flow-flash experiments [57]. As to the rate of protonic phase 1, it is pH-independent which may indicate that the phase is rate limited by internal proton transfer step. The pH-dependence of the two protonic electrogenic phases is in good agreement with the pH-dependence of the two phases of heme *a* reoxidation reported for the $\mathbf{F_{II}} \rightarrow \mathbf{O}$ transition induced by single-electron photoreduction of bovine enzyme [58].

Both protonic phases reveal high activation energies of 17–19 kcal/mol which is much higher than ~12 kcal/mol reported for the $\mathbf{F} \rightarrow \mathbf{O}$ transition in the flow-flash studies of bovine [57] or bacterial COX [59].

Interestingly, while there are two protonic electrogenic phases coupled to ET from heme *a* to heme a_3, reoxidation of heme *a* measured spectrophotometrically under the same conditions, either in solution or in proteoliposomes (black and red traces in Fig. 3A), is essentially monophasic (75–90%) with τ of ~1.4 ms at pH 8 [50]. Accordingly, 82% of heme *a* is reoxidized with τ of ca. 2 ms in the single electron photoreduction-induced $\mathbf{F_{II}} \rightarrow \mathbf{O}$ transition in mitochondrial COX [58].

As shown in Fig. 3A, the electrogenic proton transfer in the $\mathbf{F_{II}} \rightarrow \mathbf{O}$ transition clearly lags behind ET from heme *a* to the ferryl-oxo complex of a_3. In other words, it is the intermediate electrogenic phase (protonic phase 1) which matches kinetically reoxidation of heme *a*, whereas protonic phase 2 takes place when ET is essentially over. The same kinetic divergence of charge translocation and ET is observed for the $\mathbf{F_I} \rightarrow \mathbf{F_{II}}$ step in the mitochondrial oxidase (see below, [39]), but not for the $\mathbf{F_{II}} \rightarrow \mathbf{O}$ transition in bacterial COX (ref. [41], Fig. 3B).

4.1.2. Bacterial A-class oxidases

A very similar picture of electrogenic events was found for the $\mathbf{F_{II}} \rightarrow \mathbf{O}$ transition in liposome-reconstituted oxidase from *R. sphaeroides* (experiments in collaboration with Bob Gennis' lab in UIUC) [40]. The microsecond phase, is followed by slower KCN-sensitive part of the response comprised of two major phases of about equal magnitude (Table 1) if serial sequence of the phases is taken into account [39]. The rate constants of all the 3 phases (ca. 15 μs, 0.4 ms and 1.5 ms [40]) are ~3-fold faster than in the bovine oxidase, which correlates with ca. 3-fold higher turnover rate of the bacterial enzyme. The results on *R. sphaeroides* have been corroborated by experiments of the Frankfurt group with COX from *P. denitrificans* [38]. Notably, contribution of the KCN-insensitive part of the response associated with reduction of heme *a* is markedly higher in the bacterial oxidases from either *R. sphaeroides* or *P. denitrificans* (~30% vs 20% in bovine enzyme, Table 1). As shown recently [42], the ~15 μs

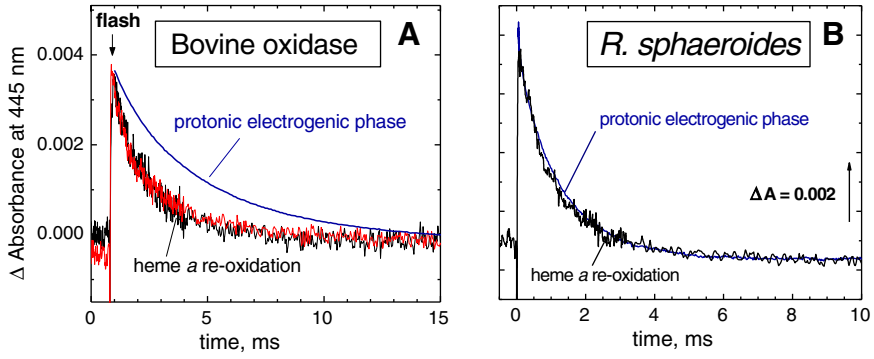

Fig. 3. Kinetics of electrogenic proton transfer and heme *a* oxidation in the $\mathbf{F_{II}} \rightarrow \mathbf{O}$ transition in the mammalian (A) and bacterial (B) cytochrome c oxidases. The data are shown for the $\mathbf{F_{II}} \rightarrow \mathbf{O}$ transition induced by single-electron photoreduction of ferryl-oxo state by RuBpy at pH 8. (A) In the bovine oxidase, KCN-sensitive electrogenic proton transfer (blue curve) lags behind reoxidation of the photoreduced heme *a* measured at 445 nm either in solubilized (black curve) or liposome-reconstituted COX (red curve) (unpublished data of S. Siletsky, [50]). (B) In *R. sphaeroides* oxidase, electrogenic proton transfer matches kinetically reoxidation of heme *a* (modified from Ref. [41], and cf. Ref. [42] for refined analysis of the data). For experimental details, see Refs. [13,41,50].

Table 4
Charge translocation phases coupled to $\mathbf{F_{II}} \rightarrow \mathbf{O}$ transition of cytochrome oxidase from *R. sphaeroides* (modified from [42]).

Electrogenic phase		τ	Contribution		Nature of the phase
			a.u.	Charges across the membrane[b]	
1	Insensitive to KCN	10 μs	1.0	0.33	Vectorial ET transfer $Cu_A \rightarrow$ heme *a*
2	Insensitive to KCN	40 μs	0.67	0.22	Internal H^+ transfer; polarization of water chain from E286 to PLS? Proton release from PLS to the P-phase? (see the text).
3	KCN-sensitive[a]	0.4 ms	1.9	0.63	Uptake of H^+_{pumped}
4	KCN-sensitive[a]	1.6 ms	2.2	0.73	Uptake of $H^+_{chemical}$ coupled to release of H^+_{pumped} from PLS to the outside
			Σ = 5.7	Σ = 1.9	

Note that whereas both KCN-insensitive components of the rapid electrogenic phase (phases 1 and 2) are coupled to reduction of heme *a*, only phase 1 corresponds to $Cu_A \rightarrow$ heme *a* vectorial ET per se.
[a] Contributions of the protonic phases calculated from the original apparent values [40] taking into account serial sequence of the two protonic phases [39].
[b] Calculated assuming that the Cu_A to heme *a* electron transfer corresponds to translocation of 1 elementary charge across 1/3 of the insulating dielectric layer [3].

KCN-insensitive part of charge translocation in bacterial COX is not homogenous and may include an internal proton transfer step in addition to vectorial electron transfer from Cu_A to heme *a* (Table 4).

In contrast to bovine enzyme (Fig. 3A), the two protonic phases in *R. sphaeroides* COX coupled to ET from heme *a* to heme a_3 match two phases of heme *a* reoxidation measured spectrophotometrically (Fig. 3B, and cf. refined analysis of the data [41] in Ref. [42]).

Availability of the mutants with amino acid replacements in the protonic channels allowed to make several important conclusions with respect to the nature of the electrogenic events coupled to the $\mathbf{F_{II}} \rightarrow \mathbf{O}$ step.

First, it was established that electrogenic uptake of both pumped and chemical protons coupled to single-electron photoreduction of the ferryl-oxo state occurs via the D-channel, while blocking the K-channel does not affect the electrogenic response any significantly [40]. Moreover, even under multiple turnover conditions transfer of the 3rd and 4th electrons in the catalytic cycle (i.e., the peroxidase half of the catalytic cycle, Fig. 1 [8,60]) does not require the K-channel, but is fully dependent on proton delivery through the D-channel [12].

Another important finding is that E286Q replacement at the intramembrane end of the D-channel eliminates all proton transfer steps that follow reduction of heme *a* [40], suggesting that intraprotein H^+ transfer to either to PLS or to the binuclear site requires protonated carboxylate of E286 as the proton donor.

At the same time, partial step of intraprotein H^+ transfer from E286 to the binuclear site (ca. 15% of charge translocation across the membrane) has been resolved for the $\mathbf{F_{II}} \rightarrow \mathbf{O}$ transition in the non-pumping N139L mutant blocked near the mouth of the D-channel [42] (see Fig. 4). A minor KCN-sensitive phase of electrogenic intraprotein H^+ transfer with $\tau \sim 0.5$ ms following reduction of heme *a* has been resolved also for D132N mutant of *R. sphaeroides* oxidase [40] The phase is very much faster than turnover of the D132N mutant and hence is not likely to report transfer of the chemical proton from E286 to the binuclear site as in the case of the N139L mutant [42]. The time constant of the residual protonic phase in D132N matches τ value of protonic phase 1 in the wild type oxidase and therefore may be associated rather with proton transfer from E286 to PLS (but not further, cf. [24]) in this non-pumping mutant.

Is it a chemical or pumped H^+ which moves first? It is natural to propose that the two protonic electrogenic phases of about equal amplitude in the $\mathbf{F_{II}} \rightarrow \mathbf{O}$ transition coupled to ET from heme *a* to the binuclear site correspond primarily to uptake of the pumped and chemical protons (e.g., [61]), although both phases include minor additional contributions from other processes. In particular, protonation of BNC is in all probability coupled to and merges into a single phase with extrusion of the pumped proton from PLS to the *P*-phase as proposed by P. Rich [62] and substantiated by theoretical calculations in Ref. [63] (see legends to Fig. 2 and Fig. 5). An obvious question is which of the two protons moves first. As postulated in the original model [17,19] (Fig. 2), the pumped proton is to be taken up before the chemical one. The question was solved experimentally by studying a mutant of *R. sphaeroides* oxidase with N139D replacement at the neck of the D-channel [41]. In the N139D mutant, catalytic activity is fully retained or even enhanced but proton pumping is absent [64]. Accordingly, the total voltage generated during the $\mathbf{F_{II}} \rightarrow \mathbf{O}$ transition in this mutant corresponds to about half that observed with the wild type oxidase [41], and of the two protonic electrogenic phases resolved in the WT oxidase only one is retained in the mutant. Conceivably, this only phase represents uptake of the "chemical" proton from the *N*-phase to the oxygen reducing site (Fig. 4).

Transfer of the pumped and chemical protons in the bacterial COX is known to differ significantly in H_2O/D_2O KIE and can be discriminated on this basis [61,65]. High H_2O/D_2O KIE of the residual protonic phase in N139D matches the KIE measured for the slow electrogenic phase (protonic phase 2) in the wild type COX [41]. Accordingly, the time constant of the sole protonic electrogenic phase in the $\mathbf{F_{II}} \rightarrow \mathbf{O}$ transition of N139D mutant oxidase fits exactly to the turnover number of the enzyme [41,64] (protonic phase 2 of the $\mathbf{F_{II}} \rightarrow \mathbf{O}$ step is known to match kinetically turnover number in either bacterial or mitochondrial COX).

Thus, in the wild type oxidase, the intermediate electrogenic phase (protonic phase 1) missing in the non-pumping mutant N139D is associated with uptake of the pumped H^+ and the slow electrogenic

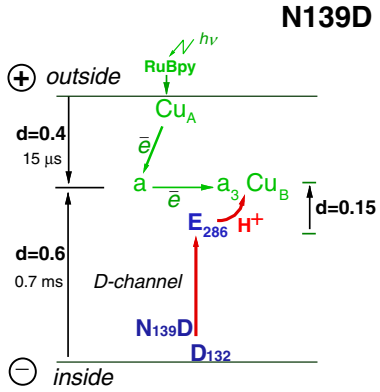

Fig. 4. Electrogenic steps coupled to transfer of the 4th electron in the non-pumping oxidase. The scheme shows partial electrogenic steps coupled to the $\mathbf{F_{II}} \rightarrow \mathbf{O}$ transition in the non-pumping fully active N139D mutant of *R. sphaeroides* oxidase [41]. Not denoted in the figure, heme a_3 is meant to be in the ferryl-oxo state prior to the flash. Movement of the chemical proton begins with H^+ transfer from E286 to the binuclear site (this minor partial electrogenic step has been resolved in the non-pumping 9% active mutant N139L [42]) followed by reprotonation of E286 from the N-phase. The microsecond electrogenic phase coupled to reduction of heme *a* and responsible for ~40% of transmembrane charge transfer may include contribution of internal proton transfer in addition to vectorial ET from Cu_A to heme *a* [42] (see Table 4 and the text).

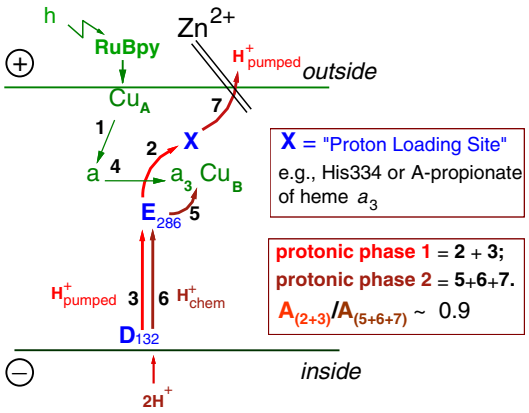

Fig. 5. Electrogenic steps coupled to transfer of the 4th electron in the pumping oxidase. The scheme shows major partial electrogenic steps resolved by single-electron photoreduction experiments for the $\mathbf{F_{II}}\rightarrow\mathbf{O}$ transition. Although not depicted in the figure, heme a_3 is meant to be in the ferryl-oxo state prior to the flash. During the $\mathbf{F_{II}}\rightarrow\mathbf{O}$ step, both the pumped and chemical protons are delivered from the *N*-phase sequentially via the D-channel. The partial steps 2 and 3 merge to form electrogenic protonic phase 1 (bright red), and the steps 5, 6 and 7 merge into electrogenic protonic phase 2 (brownish red). The sequence of events differs from the original scheme in Fig. 2 [17] by order of the partial steps in two cases as described in the text and in the legend to Fig. 2. Proton exit from PLS to the outer phase is depicted to be inhibited by Zn ions from the outside of liposomes, which results in deceleration of the overall protonic phase 2 [47]. The magnitude ratio of the protonic phases 1 and 2, $A_{(2+3)}/A_{(5+6+7)}$ ~0.9, is consistent with "electrical" location of the groups considered in the membrane dielectric as calculated in Ref. [69].

phase (protonic phase 2) with uptake of the chemical H^+ (coupled to extrusion of the pumped H^+ from PLS to the outside [62,63]). Hence, transfer of the H^+_{pumped} precedes uptake of the $H^+_{chemical}$. This finding confirmed the prediction of the model in Fig. 2 and has been supported by theoretical considerations [48,66] as well as by experiments on *P. denitrificans* oxidase [67] (but see Refs. [65,68] for an alternative view of the problem). That the pumped proton is taken up before the chemical has been concluded also for the "$\mathbf{O_H}$"$\rightarrow\mathbf{R^1}$ transition in bacterial COX from *P. denitrificans* [37,69].

Sequence of the events during the $\mathbf{F_{II}}\rightarrow\mathbf{O}$ transition in the pumping COX emerging from the time-resolved single-electron photoreduction studies correlated with the 3D structure of COX and particularly with theoretical prediction of the two water chains enabling protonic connection of $E286_{rs}$ ($E242_{bt}$) with PLS and BNC [70,71] is shown schematically in Fig. 5. The scheme is analogous to the model considered in Ref. [72], and comprises the same major steps as proposed in the original model [17] (Fig. 2) except that the order of the partial steps has been reversed in two cases.

Notably, the sequence of the partial steps may be different for the $\mathbf{F_{II}}\rightarrow\mathbf{O}$ transition observed during oxidation of the fully reduced COX by oxygen due to different properties of the ferryl-oxo state formed in the two experimental approaches, as pointed out in Ref. [65] and discussed below.

4.2. Transfer of the 3rd electron; $\mathbf{F_I}\rightarrow\mathbf{F_{II}}$ ("$\mathbf{P_M}$"$\rightarrow\mathbf{F}$) transition

Charge translocation events coupled to transfer of the 3rd electron ($\mathbf{F_I}\rightarrow\mathbf{F_{II}}$ step) were also time-resolved originally for the bovine oxidase [31]. First of all, side-by-side experiments with the same preparation of liposome-reconstituted bovine COX allowed to establish that the number of charges translocated across the membrane during the $\mathbf{F_I}\rightarrow\mathbf{F_{II}}$ and $\mathbf{F_{II}}\rightarrow\mathbf{O}$ single-electon steps is the same [31]. Electrogenic phases of equal magnitude were found to be associated with the "$\mathbf{P_R}$"$\rightarrow\mathbf{F_{II}}$ and $\mathbf{F_{II}}\rightarrow\mathbf{O}$ ("$\mathbf{O_H}$"?) transitions during oxidation of the fully reduced bovine oxidase by O_2 [73], although these transitions may not be considered as direct counterparts of the $\mathbf{F_I}\rightarrow\mathbf{F_{II}}$ and $\mathbf{F_{II}}\rightarrow\mathbf{O}$ steps in the single-electron photoreduction studies.

In bovine oxidase, the patterns of charge translocation coupled to the single-electron steps $\mathbf{F_I}\rightarrow\mathbf{F_{II}}$ and $\mathbf{F_{II}}\rightarrow\mathbf{O}$ are very similar (Table 1), except that both protonic phases coupled to transfer of the 3rd electron (τ values of ~0.3 ms and ~1.5 ms) are 2–3-fold faster than observed for transfer of the 4th electron.

In both cases, there is rapid electrogenic phase coupled to reduction of heme *a* with τ of 40–50 μs and contribution of ~20%; this phase is followed by two KCN-sensitive protonic phases of similar magnitudes ([protonic phase 1]/[protonic phase 2] = 0.8–0.9) (Table 1). Both in the $\mathbf{F_I}\rightarrow\mathbf{F_{II}}$ and $\mathbf{F_{II}}\rightarrow\mathbf{O}$ steps, the first of the two protonic phases is concomitant with almost complete oxidation of heme *a* by heme a_3, whereas the second protonic phase occurs largely after completion of the heme absorption changes (cf. [39] and Fig. 3A).

A comparative scheme of the two single-electron transitions ($\mathbf{F_I}\rightarrow\mathbf{F_{II}}$ and $\mathbf{F_{II}}\rightarrow\mathbf{O}$) constituting the peroxidase phase of the catalytic cycle is shown in Fig. 6. It is tempting to propose, that uptake of the chemical proton (and coupled release of the pumped proton from PLS) are driven by protein relaxation following ET from heme *a* to heme a_3, in agreement with a classical concept of membrane-bound redox energy-transducer [74].

A limited number of experiments were made on the $\mathbf{F_I}\rightarrow\mathbf{F_{II}}$ transition in the bacterial oxidases from *R. sphaeroides* [39] and *P. denitrificans* [36] and the data for the two enzyme species are in good agreement. A rapid part of charge translocation coupled to reduction of heme *a* with τ of 13–15 μs [39] or 10 μs [36] is similar to the rapid phase observed in the $\mathbf{F_{II}}\rightarrow\mathbf{O}$ transition. The initial charge translocation step is followed by two protonic phases with τ values of 0.18 and 0.85 ms in *R. sphaeroides* oxidase [39] or 0.12 and 0.97 ms in *P. denitrificans* enzyme [36]. The phases are 2–3-fold faster than the corresponding steps in the $\mathbf{F_{II}}\rightarrow\mathbf{O}$ transition, like it is observed for the mitochondrial enzyme [31].

However, in contrast to the results obtained with the bovine oxidase, the relative amplitudes of the two protonic phases in the

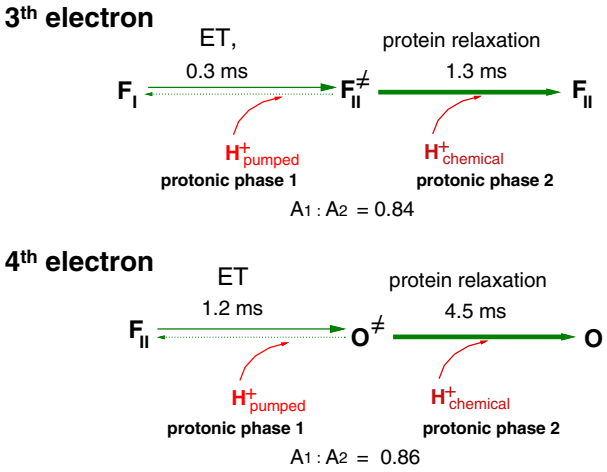

Fig. 6. Common pattern of the $\mathbf{F_I}\rightarrow\mathbf{F_{II}}$ and $\mathbf{F_{II}}\rightarrow\mathbf{O}$ transitions in bovine oxidase. The patterns of electrogenic proton translocation coupled to transfer of the 3rd and 4th electrons are very similar in the mitochondrial oxidase, except that the protonic phases 2 and 3 in the $\mathbf{F_I}\rightarrow\mathbf{F_{II}}$ are 3–4 fold faster. In both cases, ET from heme *a* to heme a_3 is coupled to protonic phase 1 (the intermediate electrogenic phase), whereas protonic phase 2 (the slow electrogenic phase) takes place after ET is essentially over (cf. Fig. 3A in this work for the $\mathbf{F_{II}}\rightarrow\mathbf{O}$ step and Fig. 4 in Ref. [39] for the $\mathbf{F_I}\rightarrow\mathbf{F_{II}}$ transition). ET to the binuclear site generates the intermediates with non-equilibrium state of the protein surroundings around the binuclear site (denoted by symbol ≠), relaxation of which to the stable configuration (e.g., ligand dissociation/association from/with Cu_B as one of the possibilities [108]) drives transfer of the chemical proton to BNC and release of the pumped proton from PLS. The scheme corresponds to a generic model of ET-driven energy-transduction proposed by DeVault [74] and extended later on to the "cubic" scheme of proton pumping by COX [78,109]. That protonic phases 1 and 2 in bovine oxidase correspond essentially to uptake of the pumped and chemical protons, respectively, is assumed by analogy with the results obtained for *R. sphaeroides* oxidase (see the text).

$\mathbf{F_I \rightarrow F_{II}}$ step in the bacterial enzyme are no longer close to each other as observed for the $\mathbf{F_{II} \rightarrow O}$ transition. The (protonic phase 1)/(protonic phase 2) magnitude ratio for the $\mathbf{F_I \rightarrow F_{II}}$ transition is 2.3 in *R. sphaeroides* oxidase [39] and 2.2 for enzyme from *P. denitrificans* [36], while it is ~0.9 for the $\mathbf{F_{II} \rightarrow O}$ step (Table 1). If we assume that the overall number of charges translocated across the membrane in the $\mathbf{F_{II} \rightarrow O}$ and $\mathbf{F_I \rightarrow F_{II}}$ transitions in the bacterial enzyme is the same as shown for the mitochondrial oxidase [31], the finding may indicate that in the bacterial oxidases, distribution of the partial proton transfer steps is very different for the $\mathbf{F_I \rightarrow F_{II}}$ and $\mathbf{F_{II} \rightarrow O}$ transitions. This is in contrast to the mitochondrial oxidase, where the magnitude ratio for the two protonic phases is very similar (0.84 and 0.86) for the $\mathbf{F_I \rightarrow F_{II}}$ and $\mathbf{F_{II} \rightarrow O}$ steps (Table 1, Fig. 6). In the $\mathbf{F_I \rightarrow F_{II}}$ transition of the bacterial enzyme, protonic phase 2 comprises less than 1/3 of the overall charge translocation coupled to oxidation of heme *a*. Such a low contribution of protonic phase 2 might indicate movement of both $H^+_{chemical}$ and H^+_{pumped} in protonic phase 1, preceding slower release of the pumped proton from PLS (protonic phase 2) (cf. the proton uptake/release data for the "$\mathbf{P_R}$" $\rightarrow \mathbf{F_{II}}$ transition in the flow-flash experiments [65]).

4.3. Photoinjection of the 1st electron ($\mathbf{O \rightarrow E}$, $\mathbf{O \rightarrow R^1}$, "$\mathbf{O_H}$" $\rightarrow \mathbf{R^1}$ transitions)

The situation is more complicated in case of addition of the 1st electron to the oxidized COX. The initial oxidized state, **O**, is notorious for multiple forms, differing in characteristics of the binuclear site [3,75]. Accordingly, the photoinjected electron may not have a well defined unique ultimate acceptor, but rather it equilibrates among three relatively high-potential acceptors: heme *a*, heme a_3 and Cu_B. Besides, it is not so easy to warranty the completely oxidized state of liposome-reconstituted COX in the presence of RuBpy and aniline even at dim light.

In the *as isolated* (or *resting*) oxidized state, photoinjection of an electron gives rise to a single microsecond electrogenic phase matching electron transfer from Cu_A to heme *a*, and there are no further ET or charge translocation events on a time-scale compatible with enzyme turnover as shown initially for the mitochondrial oxidase [31,58]. These results were questioned by Ruitenberg et al. [33] who observed some KCN-sensitive protonic phase upon single electron reduction of the oxidized COX from *P. denitrificans*. The phase was assigned to proton uptake via the K-channel. However, subsequent experiments of Helsinki group [35,76] did not reproduce this observation and confirmed the initial findings in [31]. According to [35], the 150 μs electrogenic phase of proton uptake via the K-channel observed in Ref. [33] could originate in the presence of singly-reduced COX in the "oxidized" sample, so that it was delivery of the *second* electron in this fraction of COX which induced the 150 μs protonic phase. Such an explanation is consistent with a relatively low amplitude of the protonic phase observed in [33] (Table 1). Alternatively, the preparations of *P. denitrificans* COX oxidase might vary between the two labs, so that in the samples used in [33] partial electron transfer of the 1st electron from heme *a* to the binuclear site did take place indeed.

That the electron photoinjected into the resting oxidized COX stays at heme *a* and does not go to the binuclear site, is often explained by low E_m value of heme a_3 in the "resting" oxidase (e.g. [77]). This is in contradiction with the data of equilibrium redox titrations, in which E_m values of the hemes *a* and a_3 are very close to each other [78,79]. One possibility is that rapid ET to heme a_3 needs to be charge compensated by proton uptake to the binuclear site, while the proton channel K required for proton delivery is closed yet in the **O** state, so that slow equilibration with protons is possible on a time-scale of redox titrations (minutes), but not on a timescale of enzyme turnover (few ms). Interestingly, the situation is different for ba_3 oxidase from *T. thermophilus*, where E_m of heme a_3 at pH below ~7.5 is more positive than that of the low-spin heme *b* [77], so that the electron injected into the oxidized enzyme goes rapidly from heme *b* to heme a_3 [80,81] (cf. also Ref. [82]) and a 250 μs KCN-sensitive protonic phase corresponding to proton uptake from the *N*-phase is observed even at pH 8 [32] (Table 1).

The situation becomes different in the case of the so-called "$\mathbf{O_H}$" state generated upon oxidation of the fully reduced COX by O_2 [76]. Unfortunately, no spectroscopic differences between the **O** and "$\mathbf{O_H}$" states have been found so far, but electron affinity of Cu_B is likely to be much higher in the "$\mathbf{O_H}$" than in the **O** state [37,82]. Accordingly, high-potential Cu_B serves as a preferred ultimate electron acceptor for the photoinjected electron in "$\mathbf{O_H}$" intermediate [37,82,83] (but, see [84]). Nevertheless, complete oxidation of heme *a* by the bincuclear site does not occur in all the "$\mathbf{O_H}$" samples as noted by the authors [37,83], and more experiments are required to clarify the phenomenon. In particular, it remains to be established whether the "$\mathbf{O_H}$" state is formed under any conditions other than oxidation of the fully reduced COX by O_2.

For "good" preparations of "$\mathbf{O_H}$", 4 electrogenic phases have been resolved in [36,37] with the characteristics given in rows 1 and 2 of Table 5. It is noted that independent fitting of the same data performed in Ref. [69] without assignment of the fixed $\tau = 10$ μs value to the first phase as done in Refs. [36,37] but probing different τ values for the phase, gave somewhat different results (Table 5, row 3). In particular, a better fit is obtained if contribution of the first phase increases to ~20% similar to the value found for the $\mathbf{F_{II} \rightarrow O}$ and $\mathbf{F_{II} \rightarrow F_I}$ transition in experiments with bovine oxidase [13,39] (cf. Table 1). The interpretation is also complicated by the fact that the last electrogenic phase is not associated with absorption changes and at the same time is slower than the enzyme turnover ($\tau = 2.6$–5.3 ms vs. ca. 1–1.5 ms typical of the enzyme turnover at this pH). If the last phase corresponds to slow release of the proton from the PLS as proposed in [37], it may be viewed as kinetically dissociated part of the slow electrogenic phase (protonic phase 2) observed in the $\mathbf{F_{II} \rightarrow O}$ transition in *R. sphaeroides* or *P. denitrificans* oxidase [38,40,42]. In such a case, the magnitude ratio of the KCN-sensitive protonic phases 1 and 2 in the "$\mathbf{O_H}$" $\rightarrow \mathbf{R^1}$ transition will constitute ~0.9, in excellent agreement with the data for the $\mathbf{F_{II} \rightarrow O}$ step in either mitochondrial or bacterial oxidase (Tables 2 and 3), and very different from the ratio of 2.3 observed for the 3rd electron in *R. sphaeroides* [39] and *P. denitrificans* oxidase [36].

Table 5
Electrogenic phases coupled to the "$\mathbf{O_H}$" $\rightarrow \mathbf{R^1}$ transition in aa_3 COX from *P. denitrificans*.

Source of the data	Phase 1 coupled to reduction of heme *a*;	Phases coupled to reoxidation of heme *a*		
		Phase 2	Phase 3	Phase 4
Verkhovsky et al. [36]	10 μs[a]; 10%	110 μs; 28%	770 μs; 46%	5.3 ms; 16%
Belevich et al. [37]	10 μs[a]; 12%	150 μs; 42%	800 μs; 30%	2.6 ms; 16%
Belevich et al. [37] as re-analyzed by Sugitani et al. [69]	20–26 μs; 17–21%[b]	140–190 μs; 36–39%	640–820 μs; 24–28%	2.2–2.4 ms; 16–19%

[a] Fixed τ value of 10 μs has been assigned during the curve fitting.
[b] Fixed value for τ of phase 1 has been varied in the range indicated and the magnitude has been corrected for incomplete ET Cu_A→heme *a*.

4.4. Photoinjection of the 2nd electron. $\mathbf{R^1 \rightarrow R^2}$ ($\mathbf{E \rightarrow R^2}$) transition

There are but very few data on the electrogenic events coupled to the $\mathbf{R^1 \rightarrow R^2}$ transition in *P. denitrificans* COX and the results are not yet quite clear. On one hand, there may be a single 150–200 μs protonic phase corresponding to uptake of protons from the N-phase via the K-channel (cf. Refs. [33] and [35]). On the other hand, ingenious generation of the $\mathbf{R^1}$ state at a rather high yield in Ref. [38] allowed the authors to observe an electric response coupled to injection of the 2nd electron consisting of the rapid, intermediate and slow phases with time constants (27 μs, 0.2 ms, and 1.5 ms) and magnitude ratios rather similar to those observed for the $\mathbf{F_{II} \rightarrow O}$ transition (Table 1). The slow but not the intermediate phase was eliminated in the non-pumping D124N_{pd} mutant. The experiments still leave space for questions as to the homogeneity of the initial and final states in the photoinduced transient. The $\mathbf{R^1}$ state generated by two-electron reduction of the ferryl-oxo complex by CO is not stable and decays gradually to CO complex of ferrous heme a_3. It is not warranted that the time course of $\mathbf{R^1}$ generation and decay controlled spectrophotometrically in Ref. [38] for the solubilized enzyme apply to the liposome-reconstituted oxidase. As discussed in Ref. [76], the $\mathbf{R^1}$-state generated by virtue of two-electron reduction of $\mathbf{F_{II}}$ by CO in Ref. [38] might be an "activated" form of $\mathbf{R^1}$ intermediate ("$\mathbf{E_H}$"). Apparently, ultimate conclusions on proton pumping coupled to transfer of the 2nd electron in the catalytic cycle ($\mathbf{R^1 \rightarrow R^2}$, $\mathbf{E \rightarrow R}$, "$\mathbf{E_H}$" → **R** transitions) would await for more experiments.

5. Electrogenic steps in *ba*$_3$-type cytochrome oxidase from *Thermus thermophilus*

ba$_3$-type cytochrome *c* oxidase from *T. thermophilus* belongs to class B of the heme-copper oxidases [15] and differs in several important respects from the A-class *aa*$_3$ oxidases from mitochondria, *R. sphaeroides* and *P. denitrificans* [85]. There are three most obvious features that imply different pumping mechanism in *ba*$_3$ oxidase.

First, there is no Mg ion in the *ba*$_3$ structure [85]. Hence, exit of the pumped proton from PLS to the *P*-phase, believed to occur via the Mg ion-associated hydrogen bond network in the bacterial A-class oxidases [23,24,86,87], should be arranged differently in *T. thermophilus ba*$_3$ oxidase (see Refs. [24,88] for recent discussion). Electrogenic proton translocation by A-class oxidases is strongly inhibited by Zn^{2+} ions binding at the high affinity site at the *outer* side of the liposome membrane [47,89]. Presumably, Zn^{2+} inhibits proton extrusion via the exit proton channel [90,91], and, simultaneously, suppresses uptake of the chemical proton, because the two processes are linked cooperatively. It is therefore interesting, that Zn^{2+} does not inhibit *ba*$_3$ oxidase, which lacks the Mg ion [47].

Second, of the three potential proton channels resolved in the structure of *ba*$_3$, there is compelling evidence only for the K-channel homologue being involved in the enzyme functioning, whereas mutations in the D-channel analog or in the Q-channel affect ET/proton translocation much less dramatically, though substantially (up to 5-fold) [92].

Third, under steady state conditions, the *ba*$_3$ oxidase has been reported to pump protons with twice lower efficiency ($H^+/e^- = 0.5$) than the A-class oxidases [93], although more experiments are required for valid conclusions. The catalytic 4-electron cycle of O_2 reduction by *ba*$_3$ oxidase is presumed to be similar to that of the A-class oxidases [94,95]. One possibility is that only two of the four single-electron steps in the catalytic cycle of *ba*$_3$ are coupled to proton pumping. Alternatively, the partial steps of the two pumped proton translocation, e.g., *N*-phase → PLS and PLS → *P*-phase, could be distributed among all the 4 redox steps [96]. Therefore, it is interesting to figure out whether some of the four single-electron steps of the *ba*$_3$ catalytic cycle may be less electrogenic than the others.

Single electron-photoreduction experiments followed by time-resolved electrometric and absorption measurements were carried out with *ba*$_3$ oxidase in [32] under two sets of conditions. The results can be summarized briefly as follows.

(1) *Photoinjection of a single electron into the oxidized ba*$_3$ (**O → R**^{1} *step)*. Under these conditions, the KCN-insensitive electrogenic phase with τ ~20 μs is followed by partial ET from heme *b* to the binuclear site coupled to electrogenic proton transfer with τ ~0.25 ms [32]; a minor additional 10 ms phase (~15%) not associated with optical changes [82] may be an artifact. The magnitude of the 0.25 ms phase is 0.67 that of the rapid KCN-insensitive phase, associated with Cu_A → heme *b* ET (Table 1). However the photoinjected 1st electron goes to the binuclear site only partially, equilibrating between the hemes *b* and a_3 at pH 8 at the ratio of 2.3:1 [82] or 1.2:1 [77]; the latter value obtained during the equilibrium titrations may be less relevant to the conditions of rapid kinetics measurements in Ref. [32]. Accordingly, the magnitude of the 0.25 ms protonic electrogenic phase recalculates to ~70%, similar to but slightly higher than the value of ~60% obtained for $\mathbf{F_{II} \rightarrow O}$ transition in the non-pumping mutant N139D of *aa*$_3$ oxidase from *R. sphaeroides* (Table 1). Apparently, the single-electron reduction of the oxidized *ba*$_3$ is coupled to chemical proton uptake from the *N*-phase associated with ET to heme a_3 [81] but not to full transmembrane proton pumping. However, contribution of an additional weakly electrogenic step of H^+_{pumped} transfer (e.g., release of H^+ from PLS to the *P*-phase, cf. [96]) cannot be excluded.

(2) *Photoinjection of a single electron into oxidized ba*$_3$ *in the presence of excess* H_2O_2 (*"*$\mathbf{F_I \rightarrow F_{II}}$*" step)*. In the oxidized state, *ba*$_3$ oxidase reacts but very slowly with any of the heme a_3 ligands tested, including H_2O_2 [32]. However, photoinjection of a single electron opens the binuclear site for rapid interaction with exogenous H_2O_2 ($k_v \sim 2 \times 10^3\ M^{-1}\ s^{-1}$ [32]). The chemistry of the reaction has not been investigated in sufficient detail, but H_2O_2 reacting with the opened binuclear site is likely to be reduced finally to water forming Compound II-type ferryl state $\mathbf{F_{II}}$ of heme a_3 (cf. [97]).

$$[b^{2+}\ a_3^{3+}\ Cu_B^{2+}] + H_2O_2 \longrightarrow [b^{3+}\ a_3^{4+}{=}O^{2-}\ Cu_B^{2+}] + H_2O$$

Therefore, the reaction may be viewed with certain reservations as an analog of the $\mathbf{F_I \rightarrow F_{II}}$ single-electron transition induced by the photoinjected electron.

Membrane potential generation coupled to single-electron photoreduction of *ba*$_3$ in the presence of H_2O_2 includes 3 phases with $\tau_1 = 20$ μs (31%); $\tau_2 = 0.42$ ms (23%) and τ_3 (at 40 mM H_2O_2) of 11.6 ms (46%). The rate, but not the magnitude, of the 3rd phase depends linearly on H_2O_2 concentration up to at least 80 mM. As with the A-class oxidases, the first rapid phase is KCN-insensitive and is linked to reduction of the low-spin heme *b*. The 2nd and 3rd phases are fully prevented by KCN and are coupled to ET from heme *b* to the binuclear site and reduction of H_2O_2. The magnitude ratio of the phases associated with the reduction and reoxidation of the low-spin heme *b* attains a value of 1:2.2, very close to the ratio obtained for the non-pumping $\mathbf{O \rightarrow R^1}$ step and markedly less than reported for the pumping $\mathbf{F_I \rightarrow F_{II}}$ transitions in the A-class oxidases (Table 1); therefore transmembrane proton pumping coupled to this step is very unlikely. Notably, the magnitude ratio of protonic phase 1 to protonic phase 2 (~0.5) is much lower than in any of the A-class oxidases (Table 1). Thus, the electrogenic pattern of the "$\mathbf{F_I \rightarrow F_{II}}$" transition in *ba*$_3$ oxidase appears to be quite different from that of the $\mathbf{F_I \rightarrow F_{II}}$ transition in the "canonical" cytochrome oxidases of the A-class.

Finally, it is noted that time-resolved electrometric studies on the oxidation of the fully-reduced *ba*$_3$ by oxygen show that formation of

$\mathbf{F_{II}}$ in this oxidase ("$\mathbf{P_R}$" → $\mathbf{F_{II}}$) is almost twice less electrogenic than the subsequent $\mathbf{F_{II}} \rightarrow \mathbf{O}$ transition [94] and, hence, this step is unlikely to be coupled to full proton pumping.

Thus the evidence currently available favors unequal electrogenicity of the individual steps in the ba_3 cycle and allows us to suggest provisionally that these are the single electron steps of $\mathbf{R^1}$ and $\mathbf{F_{II}}$ formation (transfer of the 1st and 3rd electrons) that are less electrogenic (not fully pumping). An interesting model of alternating steps of H^+_{pumped} uptake and release in *T. thermophilus* ba_3 oxidase has been proposed recently [96]. Within a framework of such hypothesis, results of the time-resolved charge translocation studies may mean that transfer of the 1st and 3rd electron would be coupled to but weakly electrogenic steps of proton release from PLS to the *P*-phase, whereas the much more electrogenic H^+ loading to PLS from the *N*-phase occurs at the steps of the 2nd and 4th electron transfer.

Obviously, more experiments are required to evaluate electrogenicity of the individual single-electron transfer steps in the catalytic cycle of the B-class ba_3 oxidase from *T. thermophilus* and to explain (but, first of all, validate) the lower efficiency of proton translocation by the enzyme under multiple-turnover conditions.

6. Comparison of the charge translocation steps observed in the single electron-photoreduction studies and during oxidation of the fully reduced COX by oxygen

Time-resolved electrometric measurements combined with the flow-flash approach were used to monitor charge translocation coupled to oxidation of the fully reduced oxidase by O_2 [14]. The electrogenic response observed consists of two parts of about equal magnitude associated with the transitions "$\mathbf{P_R}$" → $\mathbf{F_{II}}$ ("$\mathbf{P_R}$" → $\mathbf{F}$) and $\mathbf{F_{II}} \rightarrow \mathbf{O}$.

6.1. The "$\mathbf{P_R}$" → $\mathbf{F}$ step

The "$\mathbf{P_R}$" → $\mathbf{F}$ and "$\mathbf{P_M}$" → $\mathbf{F}$ steps are treated sometimes as two versions of the same "$\mathbf{P} \rightarrow \mathbf{F}$" transition in the catalytic cycle [3], which may be confusing for the readers outside the area. The "$\mathbf{P_R}$" intermediate is not a counterpart of $\mathbf{F_I}$ ("$\mathbf{P_M}$") because the two intermediates are at different redox level. $\mathbf{F_I}$ ("$\mathbf{P_M}$") is Compound I-type species, two-electron deficient relative to the resting oxidized state, whereas "$\mathbf{P_R}$" is a Compound II-type intermediate, one electron deficient relative to the oxidized state. Actually, "$\mathbf{P_R}$" is at the same reduction level as intermediate $\mathbf{F_{II}}$ but lacks at least one proton, and can be denoted as $\mathbf{F_{II}}_{deprotonated}$ [42]. Therefore it is not surprising that in bovine oxidase, the pattern of electrogenic proton transfer is quite different for the "$\mathbf{P_R} \rightarrow \mathbf{F}$" transition in the flow-flash studies (a single ~80 μs phase [73]) and for the $\mathbf{F_I} \rightarrow \mathbf{F_{II}}$ transition induced by single-electron photoreduction of $\mathbf{F_I}$ (two protonic phases with τ of 0.3 and 1.3 ms [31,39], Fig. 5). A similar difference between charge translocation coupled to the "$\mathbf{P_R}$" → $\mathbf{F}$ step in the flow-flash experiments and to the $\mathbf{F_I} \rightarrow \mathbf{F_{II}}$ step in the single-electron photoreduction studies is noted for the bacterial oxidases from either *R. sphaeroides* (cf. Refs. [39] and [98]) or *P. denitrificans* (cf. Refs. [99] and [36]).

6.2. The $\mathbf{F_{II}} \rightarrow \mathbf{O}$ step

It makes more sense to compare the $\mathbf{F_{II}} \rightarrow \mathbf{O}$ transitions in the flow-flash and single-electron photoreduction experiments. The ferryl-oxo intermediates ($\mathbf{F_{II}}$, $\mathbf{F_{580}}$ or simply $\mathbf{F}$) generated during oxidation of the fully reduced COX by O_2 and upon reaction of the oxidized COX with H_2O_2 are thought to be similar if not identical. With both methods, two protonic electrogenic phases are resolved in the $\mathbf{F_{II}} \rightarrow \mathbf{O}$ transition. In case of the mitochondrial enzyme, the τ values of ~0.7 ms and ~4 ms determined for the two phases in the flow-flash experiments [73] are in reasonable agreement with the values of 1.2 and 4.5 ms found in single-electron photoreduction studies [13].

However, the two electrogenic phases resolved in the flow-flash studies for the $\mathbf{F_{II}} \rightarrow \mathbf{O}$ transition in *R. sphaeroides* COX ($\tau_1 = 0.8$ ms and $\tau_2 = 4.5$ ms at pH 8 [98]) are 2–3-fold slower than observed for the bacterial enzyme in single-electron photoreduction experiments (~0.4 ms and ~1.5 ms [40], Table 4). Peculiarly, the rates of the two protonic phases in the $\mathbf{F_{II}} \rightarrow \mathbf{O}$ transition in *R. sphaeroides* oxidase as resolved in the flow-flash experiments [98] virtually coincide with the rates of the corresponding phases in the mitochondrial oxidase (see above, [73]), whereas in the single electron-photoreduction experiments, all charge transfer steps coupled to $\mathbf{F_{II}} \rightarrow \mathbf{O}$ transition in either *R. sphaeroides* [40] or *P. denitrificans* oxidase [38] are 3–4-fold faster than for the mitochondrial oxidase. Thus there is a discrepancy also between the two sets of electrometric data for the $\mathbf{F_{II}} \rightarrow \mathbf{O}$ transition in the bacterial oxidase.

More importantly, the activation energy for the protonic electrogenic phases in the $\mathbf{F_{II}} \rightarrow \mathbf{O}$ step of bovine oxidase is 17–19 kcal/mol in the single-electron photoreduction studies (Table 3), but only ca. 12 kcal/mol in the flow-flash experiments [57]. Accordingly, low activation energy (<13 kcal/mol) has been determined for the $\mathbf{F_{II}} \rightarrow \mathbf{O}$ step in the flow-flash studies of *R. sphaeroides* oxidase [59]. Such a significant difference in E_{act} implies different rate-limiting processes inherent in the $\mathbf{F_{II}} \rightarrow \mathbf{O}$ step under the two sets of conditions.

Perhaps the most striking difference between the $\mathbf{F_{II}} \rightarrow \mathbf{O}$ transitions in the flow-flash and single electron-photoreduction studies is revealed by experiments with the *R. sphaeroides* COX mutant N139L (non-pumping, ~9% active). During oxidation of the fully reduced enzyme by O_2, the $\mathbf{F_{II}} \rightarrow \mathbf{O}$ step in the mutant is inhibited ca. 200-fold (k_v ~2 s^{-1} at pH 8), which is ~20-fold slower than steady-state enzyme turnover under these conditions and than the rate of the $\mathbf{F_{II}} \rightarrow \mathbf{O}$ transition induced in the same mutant by single-electron photoreduction of $\mathbf{F_{II}}$ [42]. The same striking discrepancy is observed for another D-channel mutant of *R. sphaeroides* COX with D132N replacement. The mutant oxidase turns over with a rate of ~30 s^{-1} at pH 8 [100], while the $\mathbf{F_{II}} \rightarrow \mathbf{O}$ step observed during oxidation of the fully reduced enzyme by O_2 is ~15-fold slower (k_v ~2 s^{-1}), as determined by single-wavelength measurements in the flow-flash studies [101,102] and confirmed by time-resolved spectra-scan experiments carried out in this group by Dr. T. Vygodina in collaborative experiments with Bob Gennis' laboratory (unpublished).

Presumably, the intermediates $\mathbf{F_{II}}$ and $\mathbf{O}$ ("$\mathbf{O_H}$") formed during the oxidation of the fully reduced oxidase by O_2 may be proton deficient relative to the intermediates $\mathbf{F_{II}}$ and $\mathbf{O}$ observed in the single-electron photoreduction studies or formed during the catalytic cycle [42].

In conclusion, charge translocation events during oxidation of the fully reduced oxidase by oxygen may not be directly comparable to the partial steps of the catalytic cycle resolved by electron photoinjection method.

7. Geometrical and electrical localization of heme *a*

It was postulated by P. Mitchell that heme *a* is located "electrically" at the middle of the mitochondrial membrane dielectric, so that redox equilibrium between cytochrome *c* and heme *a* in the CO-inhibited COX in rat liver mitochondria responds to ~50% of artificially imposed transmembrane electric potential difference of either sign [56]. Accordingly, vectorial electron transfer from Cu_A to heme *a* would be expected to account for translocation of ~0.5 elementary charges across the membrane, as presumed in the early time-resolved electrometric studies [13,73].

However, resolution of the 3D structure showed that heme *a* is located not in the middle of the membrane, but closer to the *P*-phase at ~1/3 of the spatial distance characterizing the insulating layer thickness. Besides, the dielectric constant in the enzyme domain "above" the hemes, containing many water molecules and polar groups, is expected to be significantly higher than in the hydrophobic milieu "below" the hemes. Therefore, vectorial electron transfer from

Cu_A to heme *a* may be expected to give rise to 1/3 of transmembrane charge transfer or less. Thus, the question of the "electrical location" of heme *a* in membrane still remains a matter of controversy.

Perhaps the simplest experimental model allowing us to address this question is provided by the non-pumping but fully active N139D mutant oxidase from *R. sphaeroides* [64]. (Fig. 4) Photoinjection of a single electron into $\mathbf{F_{II}}$ state of the mutant oxidase gives rise to electrogenic response comprised of only 2 major phases associated with electron transfer from Cu_A to heme *a* (and then to heme a_3) and uptake of a chemical proton required for water formation. In combination, these two electrogenic steps result in transmembrane transfer of one charge per electron. The two phases are well separated in time, so it is easy to measure directly their relative contributions and thus to determine "electrical localization" of heme *a* in the membrane. It has been found that ca. 40% of $\Delta\psi$ is coupled to heme *a* reduction step, and ca. 60% corresponds to proton uptake from the N-phase [41]. The value of ~40% is consistent with the measurements of the $\mathbf{F_{II}} \rightarrow \mathbf{O}$ and $\mathbf{F_I} \rightarrow \mathbf{F_{II}}$ transition in the mitochondrial oxidase [13,31] as well as with the experimental data obtained in [37] for the "$\mathbf{O_H}$" $\rightarrow \mathbf{R^1}$ transition in *P. denitrificans* enzyme as re-analyzed in [69]. The values around 40% have been obtained also by theoretical calculations in Ref. [69]. At the same time, calibration of the $Cu_A \rightarrow$ heme *a* electrogenicity by comparison of the electric responses coupled to oxidation of the fully reduced COX by O_2 and reversed electron flow from heme *a* to Cu_A gives a value of 33% (1/11 of 3.7 charges assumed to be translocated across the membrane during oxidation of the fully reduced COX [73,103]) exactly matching the geometrical position of Fe ion in heme *a*.

Contribution of heme *a* reduction to $\Delta\psi$ generation may be higher than implied by its geometrical position in the membrane, e.g., as it is in the case of the $\mathbf{F_{II}} \rightarrow \mathbf{O}$ transition in COX from *R. sphaeroides* [40] or *P. denitrificans* [38] oxidases (Table 1) as well as in the equilibrium measurements of Hinkle and Mitchell [56], if charge translocation coupled to heme *a* reduction is not confined to vectorial ET from Cu_A to heme *a*, but includes additional proton transfer steps as shown in [42] (Table 4).

A possibility of additional charge (H^+) transfer phase(s) coupled to reduction of heme *a* besides the vectorial ET from Cu_A to heme *a* was recognized early [13] but received experimental support only recently [42], and the nature of the additional charge movements coupled to heme *a* reduction remains to be established. It is interesting that as pointed out in Ref. [24], reduction of Cu_A can attract proton from PLS to Cu_A ligands His204 and Glu198 (bovine numbering); the mobilized proton may be then released electrogenically via the "R-pathway" [24] to the outside upon oxidation of Cu_A by heme *a*. A similar idea was considered in Ref. [23]. Hence, release of the pumped proton from PLS to the *P*-aqueous phase may be coupled under certain conditions to oxidation of Cu_A by heme *a*. This is, of course, but one of several possibilities (cf. Ref [42]).

8. Summary and conclusions

1. Time-resolved studies of charge translocation coupled to $\mathbf{F_{II}} \rightarrow \mathbf{O}$ transition in the mitochondrial and bacterial cytochrome oxidases reveal all the major partial charge transfer steps predicted by the original model of proton translocation by COX [17,19]; the results are consistent with other specific predictions of the model: transfer of the pumped proton before the chemical, and gating of ET from heme *a* to heme a_3 by transfer of the pumped proton from the bottom of the input proton channel (E286 in case of *R. sphaeroides* COX) to the bottom of the exit proton conducting pathway (proton loading site).
2. There is a tendency in the literature to seek for a uniform protonmotive mechanism common for every of the four single-electron catalytic steps in the same enzyme species, as well as for the same step in different oxidases [3,36,69] (but cf. [4,104]). It may be worthwhile to underscore experimental observations that point to the *differences* among the individual single-electron transitions.
   (a). Time-resolved pattern of charge translocation associated with the "$\mathbf{P_R}$" $\rightarrow \mathbf{F_{II}}$ and $\mathbf{F_{II}} \rightarrow \mathbf{O}$ transitions during oxidation of the fully reduced oxidase by O_2 (flow-flash studies) differs substantially from the electrogenic events coupled to transfer of the 3rd and 4th electrons in the catalytic cycle studied with the single-electron photoreduction method.
   (b). For the same single-electron transition, charge transfer mechanisms may differ in different oxidases of A-class e.g.:
      (i) In *R. sphaeroides* COX, the two phases of proton translocation in the $\mathbf{F_{II}} \rightarrow \mathbf{O}$ transition coincide with the two phases of ET from heme *a* to heme a_3, whereas in the mitochondrial COX, about half of electrogenic proton transfer (protonic phase 2) takes place after ET is over.
      (ii) In the oxidases from *R. sphaeroides* and *P. denitrificans*, contribution of the rapid electrogenic phase associated with the reduction of heme *a* during the $\mathbf{F_{II}} \rightarrow \mathbf{O}$ transition (30%) is markedly higher than in the mitochondrial oxidase (20%), presumably due to additional phase(s) of internal proton transfer coupled to vectorial ET from Cu_A to heme *a*.
      (iii) The [protonic 1]/[protonic 2] phase magnitude ratio for the $\mathbf{F_I} \rightarrow \mathbf{F_{II}}$ transition is ca. 0.9 for the mitochondrial, but 2.2–2.3 for the bacterial oxidases.
3. Charge transfer characteristics may differ for different single electron steps in the same enzyme. Thus, in *R. sphaeroides* and *P. denitrificans* COX, the [protonic phase 1]/[protonic phase 2] magnitude ratio is 0.9 for the $\mathbf{F_{II}} \rightarrow \mathbf{O}$ step, but 2.3 for the $\mathbf{F_I} \rightarrow \mathbf{F_{II}}$ step, which excludes identical sequence of partial proton transfer steps during transfer of the 3rd and 4th electrons.

Acknowledgments

The work has been supported by the Howard Hughes Medical Institute International Scholar Award 55005615 to A.A.K and the grants from Russian Fund for Basic Research (06-04-48608 and 09-04-00140 to S.A.S, and 11-04-01330 to A.A.K).

References

[1] R.B. Gennis, Coupled proton and electron transfer reactions in cytochrome oxidase, Front. Biosci. 9 (2004) 581–591.
[2] J.P. Hosler, S. Ferguson-Miller, D.A. Mills, Energy transduction: proton transfer through the respiratory complexes, Annu. Rev. Biochem. 75 (2006) 165–187.
[3] I. Belevich, M.I. Verkhovsky, Molecular mechanism of proton translocation by cytochrome *c* oxidase, Antioxid. Redox Signal. 10 (2008) 1–29.
[4] S. Yoshikawa, K. Muramoto, K. Shinzawa-Itoh, Proton-pumping mechanism of cytochrome c oxidase, Annu. Rev. Biophys. 40 (2011) 205–223.
[5] P. Mitchell, Chemiosmotic Coupling and Energy Trunsduction, Glynn Research Ltd., Bodmin, 1968.
[6] G.T. Babcock, C. Varotsis, Y. Zhang, O_2 activation in cytochrome oxidase and in other heme proteins, Biochim. Biophys. Acta 1101 (1992) 192–194.
[7] M. Sono, M.P. Roach, E.D. Coulter, J.H. Dawson, Heme-containing oxygenases, Chem. Rev. 96 (1996) 2841–2887.
[8] A. Konstantinov, Cytochrome *c* oxidase as a proton-pumping peroxidase: reaction cycle and electrogenic mechanism, J. Bioenerg. Biomembr. 30 (1998) 121–130.
[9] Y. Yoshioka, M. Mitani, B3LYP study on reduction mechanisms from O_2 to H_2O at the catalytic sites of fully reduced and mixed-valence bovine cytochrome *c* oxidases, Bioinorg. Chem. Appl. (2010) (2010) Article ID 182804.

[10] L.M. Blomberg, M.R.A. Blomberg, P.E.M. Siegbahn, A theoretical study on the binding of O_2, NO and CO to heme proteins, J. Inorg. Biochem. 99 (2005) 949–958.
[11] A.A. Konstantinov, T.V. Vygodina, N. Capitanio, S. Papa, Ferrocyanide peroxidase activity of cytochrome *c* oxidase, Biochim. Biophys. Acta 1363 (1998) 11–23.
[12] T.V. Vygodina, C. Pecoraro, D. Mitchell, R. Gennis, A.A. Konstantinov, The mechanism of inhibition of electron transfer by amino acid replacement K362M in a proton channel of *Rhodobacter sphaeroides* cytochrome *c* oxidase, Biochemistry 37 (1998) 3053–3061.
[13] D. Zaslavsky, A. Kaulen, I.A. Smirnova, T.V. Vygodina, A.A. Konstantinov, Flash-induced membrane potential generation by cytochrome *c* oxidase, FEBS Lett. 336 (1993) 389–393.
[14] M.I. Verkhovsky, J.E. Morgan, M. Verkhovskaya, M. Wikstrom, Translocation of electrical charge during a single turnover of cytochrome *c* oxidase, Biochim. Biophys. Acta 1318 (1997) 6–10.
[15] M.M. Pereira, M. Santana, M. Teixeira, A novel scenario for the evolution of haem-copper oxygen reductases, Biochim. Biophys. Acta 1505 (2001) 185–208.
[16] V.Y. Artsatbanov, A.A. Konstantinov, V.P. Skulachev, Localization of cytochrome oxidase in the coupling membrane: cytochrome *a* interaction with H^+ ions of the mitochondrial matrix, Dokl. Akad. Nauk SSSR 237 (1977) 461–464.
[17] V.Y. Artzatbanov, A.A. Konstantinov, V.P. Skulachev, Involvement of intramitochondrial protons in redox reactions of cytochrome *a*, FEBS Lett. 87 (1978) 180–185.
[18] M. Wikstrom, Proton pump coupled to cytochrome *c* oxidase in mitochondria, Nature 266 (1977) 271–273.
[19] A.A. Konstantinov, Role of protons in the mechanism of coupling site III of the mitochondrial respiratory chain: cytochrome oxidase as an electronic-protonic generator of membrane potential, Dokl. Akad. Nauk SSSR 237 (1977) 713–716.
[20] E.A. Liberman, Potential difference across the membrane of subcellular vesicles. III. Proton channels in oxidative phosphorylation, Biophysics (Moscow) 22 (1977) 1115–1128.
[21] S. Iwata, C. Ostermeier, B. Ludwig, H. Michel, Structure at 2.8 A resolution of cytochrome *c* oxidase from *Paracoccus denitrificans*, Nature 376 (1995) 660–669.
[22] T. Tsukihara, H. Aoyama, E. Yamashita, T. Takashi, H. Yamaguichi, K. Shinzawa-Itoh, R. Nakashima, R. Yaono, S. Yoshikawa, The whole structure of the 13-subunit oxidized cytochrome c oxidase at 2.8 A, Science 272 (1996) 1136–1144.
[23] M.A. Sharpe, S. Ferguson-Miller, A chemically explicit model for the mechanism of proton pumping in heme-copper oxidases, J. Bioenerg. Biomembr. 40 (2008) 541–549.
[24] R. Sugitani, A.A. Stuchebrukhov, Molecular dynamics simulation of water in cytochrome c oxidase reveals two water exit pathways and the mechanism of transport, Biochim. Biophys. Acta 1787 (2009) 1140–1150.
[25] J. Koepke, E. Olkhova, H. Angerer, H. Muller, G. Peng, H. Michel, High resolution crystal structure of *Paracoccus denitrificans* cytochrome c oxidase: new insights into the active site and the proton transfer pathways, Biochim. Biophys. Acta 1787 (2009) 635–645.
[26] T. Nilsson, Photoinduced electron transfer from Tris(2,2′-bipyridyl)ruthenium to cytochrome *c* oxidase, Proc. Natl. Acad. Sci. U. S. A. 89 (1992) 6497–6501.
[27] L.A. Drachev, A.D. Kaulen, V.P. Skulachev, Time resolution of the intermediate steps in the bacteriorhodopsin-linked electrogenesis, FEBS Lett. 87 (1978) 161–167.
[28] L.A. Drachev, A.D. Kaulen, L.V. Khitrina, V.P. Skulachev, Fast stages of photoelectric processes in biological membranes. I. Bacteriorhodopsin, Eur. J. Biochem. 117 (1981) 461–470.
[29] O.P. Kaminskaya, L.A. Drachev, A.A. Konstantinov, A.Y. Semenov, V.P. Skulachev, Electrogenic reduction of the secondary quinone acceptor in chromatophores of *Rhodospirillum rubrum*, FEBS Lett. 202 (1986) 224–228.
[30] S.M. Dracheva, L.A. Drachev, A.A. Konstantinov, A.Y. Semenov, V.P. Skulachev, A.M. Arutjunjan, V.A. Shuvalov, S.M. Zaberezhnaya, Electrogenic steps in the redox reactions catalyzed by photosynthetic reaction-center complex in *Rhodopseudomonas viridis*, Eur. J. Biochem. 171 (1988) 253–264.
[31] S. Siletsky, A.D. Kaulen, A.A. Konstantinov, Resolution of electrogenic steps coupled to conversion of cytochrome c oxidase from the peroxy to the ferryl-oxo state, Biochemistry 38 (1999) 4853–4861.
[32] S. Siletskiy, T. Soulimane, N. Azarkina, T.V. Vygodina, G. Buse, A. Kaulen, A. Konstantinov, Time-resolved generation of membrane potential by ba_3 cytochrome c oxidase from *Thermus thermophilus*. Evidence for reduction-induced opening of the binuclear centre, FEBS Lett. 457 (1999) 98–102.
[33] M. Ruitenberg, A. Kannt, E. Bamberg, B. Ludwig, H. Michel, K. Fendler, Single-electron reduction of the oxidized state is coupled to proton uptake via the k pathway in *Paracoccus denitrificans* cytochrome *c* oxidase, Proc. Natl. Acad. Sci. U. S. A. 97 (2000) 4632–4636.
[34] M.K.F. Wikstrom, A. Jasaitis, C. Backgren, A. Puustinen, M.I. Verkhovsky, The role of the D- and K-pathways of proton transfer in the function of the haem-copper oxidases, Biochim. Biophys. Acta 1459 (2000) 514–520.
[35] M.I. Verkhovsky, A. Tuukkanen, C. Backgren, A. Puustinen, M. Wikstrom, Charge translocation coupled to electron injection into oxidized cytochrome *c* oxidase from *Paracoccus denitrificans*, Biochemistry 40 (2001) 7077–7083.
[36] M.I. Verkhovsky, I. Belevich, D.A. Bloch, M. Wikstrom, Elementary steps of proton translocation in the catalytic cycle of cytochrome oxidase, Biochim. Biophys. Acta 1757 (2006) 401–407.
[37] I. Belevich, D.A. Bloch, M. Wikstrom, M.I. Verkhovsky, Exploring the proton pump mechanism of cytochrome *c* oxidase in real time, Proc. Natl. Acad. Sci. U. S. A. 104 (2007) 2685–2690.
[38] M. Ruitenberg, A. Kannt, E. Bamberg, K. Fendler, H. Michel, Reduction of cytochrome c oxidase by a second electron leads to proton translocation, Nature 417 (2002) 99–102.
[39] S.A. Siletsky, D. Han, S. Brand, J.E. Morgan, M. Fabian, L. Geren, F. Millett, B. Durham, A.A. Konstantinov, R.B. Gennis, Single-electron photoreduction of the P_M intermediate of cytochrome c oxidase, Biochim. Biophys. Acta 1757 (2006) 1122–1132.
[40] A.A. Konstantinov, S. Siletsky, D. Mitchell, A. Kaulen, R.B. Gennis, The roles of the two proton input channels in cytochrome c oxidase from *Rhodobacter sphaeroides* probed by the effects of site-directed mutations on time resolved electrogenic intraprotein proton transfer, Proc. Natl. Acad. Sci. U. S. A. 94 (1997) 9085–9090.
[41] S.A. Siletsky, A.S. Pawate, K. Weiss, R.B. Gennis, A.A. Konstantinov, Transmembrane charge separation during the ferryl-oxo → oxidized transition in a non-pumping mutant of cytochrome *c* oxidase, J. Biol. Chem. 279 (2004) 52558–52565.
[42] S.A. Siletsky, J. Zhu, R.B. Gennis, A.A. Konstantinov, Partial steps of charge translocation in the nonpumping N139L mutant of *Rhodobacter sphaeroides* cytochrome c oxidase with a blocked D-channel, Biochemistry 49 (2010) 3060–3073.
[43] T.V. Vygodina, A.A. Konstantinov, H_2O_2-induced conversion of cytochrome c oxidase peroxy complex to oxoferryl state, Ann. NY Acad. Sci. 550 (1988) 124–138.
[44] J. Wrigglesworth, Formation and reduction of a "peroxy" intermediate of cytochrome *c* oxidase, Biochem. J. 217 (1984) 715–719.
[45] M. Fabian, G. Palmer, The interaction of cytochrome oxidase with hydrogen peroxide: the relationship of compounds P and F, Biochemistry 34 (1995) 13802–13810.
[46] D.L. Zaslavsky, I.A. Smirnova, S.A. Siletskiy, A.D. Kaulen, F. Millett, A.A. Konstantinov, Rapid kinetics of membrane potential generation by cytochrome *c* oxidase with the photoactive Ru(II)–tris–bipyridyl derivative of cytochrome *c* as electron donor, FEBS Lett. 359 (1995) 27–30.
[47] S.S. Kuznetsova, N.V. Azarkina, T.V. Vygodina, S.A. Siletsky, A.A. Konstantinov, Zink ions as cytochrome c oxidase inhibitors: two sites of action, Biochem. Mosc. 70 (2005) 128–136.
[48] D.M. Medvedev, E.S. Medvedev, A.I. Kotelnikov, A.A. Stuchebrukhov, Analysis of the kinetics of the membrane potential generated by cytochrome *c* oxidase upon single electron injection, Biochim. Biophys. Acta 1710 (2005) 47–56.
[49] D.L. Zaslavskiy, Mechanism of membrane potential generation by cytochrome c oxidase. PhD Thesis, Moscow State University, Moscow (1994), pp. 1–125.
[50] S.A. Siletsky, Studies of electrogenic transfer of protons in cytochrome oxidase. PhD Thesis, Moscow State University, Moscow (1998), pp. 1–108.
[51] S. Siletsky, D. Zaslavsky, I. Smirnova, A. Kaulen, A. Konstantinov, F-to-O transition of cytochrome c oxidase: pH and temperature effects on the kinetics of charge translocation, Biochem. Soc. Trans. 28 (2000) A469.
[52] D. Zaslavsky, R.C. Sadoski, K. Wang, B. Durham, R.B. Gennis, F. Millett, Single electron reduction of cytochrome *c* oxidase compound F: resolution of partial steps by transient spectroscopy, Biochemistry 37 (1998) 14910–14916.
[53] K. Kobayashi, H. Une, K. Hayashi, Electron transfer process in cytochrome oxidase after pulse radiolysis, J. Biol. Chem. 246 (1989) 7976–7980.
[54] O. Farver, O. Einarsdottir, I. Pecht, Electron transfer rates and equilibrium within cytochrome c oxidase, Eur. J. Biochem. 267 (2000) 950–954.
[55] P. Mitchell, Chemiosmotic Coupling in Oxidative and Photosynthetic Phosphorylation, Glynn Research Ltd., Bodmin, UK, 1966.
[56] P. Hinkle, P. Mitchell, Effect of membrane potential on the redox poise between cytochrome *a* and cytochrome *c* in rat liver mitochondria, J. Bioenerg. 1 (1970) 45–60.
[57] M. Oliveberg, P. Brzezinski, B.G. Malmstrцm, The effect of pH and temperature on the reaction of fully reduced and mixed-valence cytochrome *c* oxidase with dioxygen, Biochem. Biophys. Acta 977 (1989) 322–328.
[58] R.C. Sadoski, D. Zaslavsky, R.B. Gennis, B. Durham, F. Millett, Exposure of bovine cytochrome *c* oxidase to high triton X-100 or to alkaline conditions causes a dramatic change in the rate of reduction of compound F, J. Biol. Chem. 276 (2001) 33616–33620.
[59] A.L. Johansson, S. Chakrabarty, C.B. Sioberg, M. Hogbom, A. Warshel, P. Brzezinski, Proton-transport mechanisms in cytochrome c oxidase revealed by studies of kinetic isotope effects, Biochim Biophys Acta 1807 (2011) 1083–1094.
[60] T.V. Vygodina, A.A. Konstantinov, Peroxidase activity of mitochondrial cytochrome *c* oxidase, Biochem. Mosc. 72 (2007) 1300–1310.
[61] P. Brzezinski, R.B. Gennis, Cytochrome c oxidase: exciting progress and remaining mysteries, J. Bioenerg. Biomembr. 40 (2008) 521–531.
[62] P.R. Rich, Towards an understanding of the chemistry of oxygen reduction and proton translocation in the iron-copper respiratory oxidases, Aust. J. Plant Physiol. 22 (1995) 479–486.
[63] J. Quenneville, D.M. Popovic, A.A. Stuchebrukhov, Combined DFT and electrostatics study of the proton pumping mechanism in cytochrome c oxidase, Biochim. Biophys. Acta 1757 (2006) 1035–1046.
[64] A.S. Pawate, J. Morgan, A. Namslauer, D. Mills, P. Brzezinski, S. Ferguson-Miller, R.B. Gennis, A mutation in subunit I of cytochrome oxidase from *Rhodobacter sphaeroides* results in an increase in steady-state activity but completely eliminates proton pumping, Biochemistry 41 (2002) 13417–13423.
[65] L. Salomonsson, K. Faxen, P. Adelroth, P. Brzezinski, The timing of proton migration in membrane-reconstituted cytochrome c oxidase, Proc. Natl. Acad. Sci. U. S. A. 102 (2005) 17624–17629.
[66] D.M. Popovic, A.A. Stuchebrukhov, Electrostatic study of the proton pumping mechanism in bovine heart cytochrome c oxidase, J. Am. Chem. Soc. 126 (2004) 1858–1871.
[67] I. Belevich, M.I. Verkhovsky, M. Wikstrom, Proton-coupled electron transfer drives the proton pump of cytochrome *c* oxidase, Nature 440 (2006) 829–832.
[68] P. Brzezinski, G. Larsson, Redox-driven proton pumping by heme-copper oxidases, Biochim. Biophys. Acta 1605 (2003) 1–13.
[69] R. Sugitani, E.S. Medvedev, A.A. Stuchebrukhov, Theoretical and computational analysis of the membrane potential generated by cytochrome c oxidase upon single electron injection into the enzyme, Biochim. Biophys. Acta 1777 (2008) 1129–1139.
[70] X. Zheng, D.M. Medvedev, J. Swanson, A.A. Stuchebrukhov, Computer simulation of water in cytochrome c oxidase, Biochim. Biophys. Acta 1557 (2003) 99–107.

[71] M. Wikstrom, M.I. Verkhovsky, G. Hummer, Water-gated mechanism of proton translocation by cytochrome c oxidase, Biochim. Biophys. Acta 1604 (2003) 61–65.
[72] D.M. Popovic, A.A. Stuchebryukhov, Proton pumping mechanism and catalytic cycle of cytochrome c oxidase: coulomb pump model with kinetic gating, FEBS Lett. 566 (2004) 126–130.
[73] A. Jasaitis, M.I. Verkhovsky, J.E. Morgan, M.L. Verkhovskaya, M. Wikstrom, Assignment and charge translocation stoichiometries of the electrogenic phases in the reaction of cytochrome *c* with dioxygen, Biochemistry 38 (1999) 2697–2706.
[74] D. DeVault, Theory of iron-sulfur center N-2 oxidation and reduction by ATP, J. Theor. Biol. 62 (1976) 115–139.
[75] A.J. Moody, "As prepared" forms of fully oxidised haem/Cu terminal oxidases, Biochim. Biophys. Acta 1276 (1996) 6–20.
[76] D. Bloch, I. Belevich, A. Jasaitis, C. Ribacka, A. Puustinen, M.I. Verkhovsky, M. Wikstrom, The catalytic cycle of cytochrome *c* oxidase is not the sum of its two halves, Proc. Natl. Acad. Sci. U. S. A. 101 (2004) 529–533.
[77] F.L. Sousa, A.F. Verissimo, A.M. Baptista, T.K. Soulimane, M. Teixeira, M.M. Pereira, Redox properties of *Thermus thermophilus* ba3: different electron-proton coupling in oxygen reductases? Biophys. J. 94 (2008) 2434–2441.
[78] M. Wikstrom, K. Krab, M. Saraste, Cytochrome Oxidase — A Synthesis, Academic Press, New York, 1981.
[79] E.A. Gorbikova, K. Vuorilehto, M. Wikstrom, M.I. Verkhovsky, Redox titration of all electron carriers of cytochrome *c* oxidase by Fourier transform infrared spectroscopy, Biochemistry 45 (2006) 5641–5649.
[80] O. Farver, Y. Chenc, J.A. Feec, I. Pechtb, Electron transfer among the Cu_A-, heme *b*- and a_3-centers of *Thermus thermophilus* cytochrome ba_3, FEBS Lett. 580 (2006) 3417–3421.
[81] O. Farver, S. Wherland, W.E. Antholine, G.J. Gemmen, Y. Chen, P. Pecht, J.A. Fee, Pulse radiolysis studies of temperature dependent electron transfers among redox centers in ba_3-cytochrome c oxidase from *Thermus thermophilus*: comparison of A- and B-type enzymes, Biochemistry in press (2011).
[82] S.A. Siletsky, I. Belevich, M. Wikstrom, T. Soulimane, M.I. Verkhovsky, Time-resolved O_H–E_H transition of the aberrant ba_3 oxidase from *Thermus thermophilus*, Biochim. Biophys. Acta 1787 (2009) 201–205.
[83] S.E. Brand, S. Rajagukguk, K. Ganesan, L. Geren, M. Fabian, D. Han, R.B. Gennis, B. Durham, F. Millett, A new ruthenium complex to study single-electron reduction of the pulsed O_H state of detergent-solubilized cytochrome oxidase, Biochemistry 46 (2007) 14610–14618.
[84] D. Jancura, V. Berka, M. Antalik, J. Bagelova, R.B. Gennis, G. Palmer, M. Fabian, Spectral and kinetic equivalence of oxidized cytochrome c oxidase as isolated and "activated" by reoxidation, J. Biol. Chem. 281 (2006) 30319–30325.
[85] T. Soulimane, G. Buse, G.B. Bourenkov, H.D. Bartunik, R. Huber, M.E. Than, Structure and mechanism of the aberrant ba_3-cytochrome *c* oxidase from *Thermus thermophilus*, EMBO J. 19 (2000) 1766–1776.
[86] M.A. Sharpe, M.D. Krzyaniak, S. Xu, J. McCracken, S. Ferguson-Miller, EPR evidence of cyanide binding to the Mn(Mg) center of cytochrome c oxidase: support for Cu_A-Mg involvement in proton pumping, Biochemistry 48 (2009) 328–335.
[87] V. Daskalakis, S.C. Farantos, V. Guallar, C. Varotsis, Regulation of electron and proton transfer by the protein matrix of cytochrome c oxidase, J. Phys. Chem. B. 115 (2011) 3648–3655.
[88] T. Tiefenbrunn, W. Liu, Y. Chen, V. Katritch, C.D. Stout, J.A. Fee, V. Cherezov, High resolution structure of the ba_3 cytochrome c oxidase from *Thermus thermophilus* in a lipidic environment, PLoS ONE 6 (2011) e22348.
[89] T.V. Vygodina, W. Zakirzyanova, A.A. Konstantinov, Inhibition of membrane-bound cytochrome c oxidase by zinc ions: High-affinity Zn^{2+}-binding site at the P-side of the membrane, FEBS Lett. 582 (2008) 4158–4162.
[90] D.A. Mills, B. Schmidt, C. Hiser, E. Westley, S. Ferguson-Miller, Membrane potential-controlled inhibition of cytochrome c oxidase by zinc, J. Biol. Chem. 277 (2002) 14894–14901.
[91] K. Faxen, L. Salomonsson, P. Adelroth, P. Brzezinski, Inhibition of proton pumping by zinc ions during specific reaction steps in cytochrome *c* oxidase, Biochim. Biophys. Acta 1757 (2006) 388–394.
[92] H.-Y. Chang, J. Hemp, Y. Chen, J.A. Fee, R.B. Gennis, The cytochrome ba_3 oxygen reductase from Thermus thermophilus uses a single input channel for proton delivery to the active site and for proton pumping, Proc. Natl. Acad. Sci. U. S. A. vol. 106 (2009) 16169–16173.
[93] A. Kannt, T. Soulimane, G. Buse, A. Becker, E. Bamberg, H. Michel, Electrical current generation and proton pumping catalyzed by the ba_3-type cytochrome *c* oxidase from Thermus thermophilus, FEBS Lett. 434 (1998) 17–22.
[94] S.A. Siletsky, I. Belevich, A. Jasaitis, A.A. Konstantinov, M. Wikstrom, T. Soulimane, M.I. Verkhovsky, Time-resolved single-turnover of ba_3 oxidase from *Thermus thermophilus*, Biochim. Biophys. Acta 1767 (2007) 1383–1392.
[95] I.A. Smirnova, D. Zaslavsky, J.A. Fee, R.B. Gennis, P. Brzezinski, Electron and proton transfer in the ba_3 oxidase from *Thermus thermophilus*, J. Bioenerg. Biomembr. 40 (2008) 281–287.
[96] C. von Ballmoos, R.B. Gennis, P. Adelroth, P. Brzezinski, Kinetic design of the respiratory oxidases, Proc. Natl. Acad. Sci. U S A. 108 (2011) 11057–11062.
[97] D. Zaslavsky, I.A. Smirnova, P. Brzezinski, K. Shinzawa-Itoh, S. Yoshikawa, R.B. Gennis, Examination of the reaction of fully reduced cytochrome oxidase with hydrogen peroxide by flow-flash spectroscopy, Biochemistry 38 (1999) 16016–16023.
[98] H. Lepp, P. Brzezinski, Internal charge transfer in cytochrome c oxidase at a limited proton supply: proton pumping ceases at high pH, Biochim. Biophys. Acta 1790 (2009) 552–557.
[99] C. Ribacka, M.I. Verkhovsky, I. Belevich, D.A. Bloch, A. Puustinen, M. Wikstrom, An elementary reaction step of the proton pump is revealed by mutation of tryptophan-164 to phenylalanine in cytochrome *c* oxidase from *Paracoccus denitrificans*, Biochemistry 44 (2005) 16502–16512.
[100] J.R. Fetter, J. Qian, J. Shapleigh, J.W. Thomas, A. Garcia-Horsman, E. Schmidt, J. Hosler, G.T. Babcock, R.B. Gennis, S. Ferguson-Miller, Possible proton relay pathways in cytochrome *c* oxidase, Proc. Natl. Acad. Sci. U. S. A. 92 (1995) 1604–1608.
[101] P. Adelroth, J. Hosler, Surface proton donors for the D-pathway of cytochrome c oxidase in the absence of subunit III, Biochemistry 45 (2006) 8308–8318.
[102] L. Salomonsson, G. Branden, P. Brzezinski, Deuterium isotope effect of proton pumping in cytochrome c oxidase, Biochim. Biophys. Acta 1777 (2008) 343–350.
[103] M.I. Verkhovsky, A. Jasaitis, M.L. Verkhovskaya, L. Morgan, M. Wikstrom, Proton translocation by cytochrome *c* oxidase, Nature 400 (1999) 480–483.
[104] H. Michel, Cytochrome c oxidase: catalytic cycle and mechanism of proton pumping — a discussion, Biochemistry 38 (1999) 15129–15140.
[105] C. Pecoraro, R.B. Gennis, T.V. Vygodina, A.A. Konstantinov, Role of the K-channel in the pH-dependence of the reaction of cytochrome *c* oxidase with hydrogen peroxide, Biochemistry 40 (2001) 9695–9708.
[106] S. Nagano, T.L. Poulos, Crystallographic study on the dioxygen complex of wild-type and mutant cytochrome P450cam, J. Biol. Chem. 280 (2005) 31659–31663.
[107] M.R.A. Blomberg, P.E.M. Siegbahn, G.T. Babcock, M. Wikstrom, Modeling cytochrome oxidase: a quantum chemical study of the O—O bond cleavage mechanism, J. Am. Chem. Soc. 122 (2000) 12848–12858.
[108] M. Wikstrom, Mechanism of proton translocation by cytochrome *c* oxidase: a new four-stroke histidine cycle, Biochim. Biophys. Acta 1458 (2000) 188–198.
[109] M. Wikstrom, Cytochrome c oxidase: 25 years of the elusive proton pump, Biochim. Biophys. Acta 1655 (2004) 241–247.